Feasibility Study -- Project Full Breeze

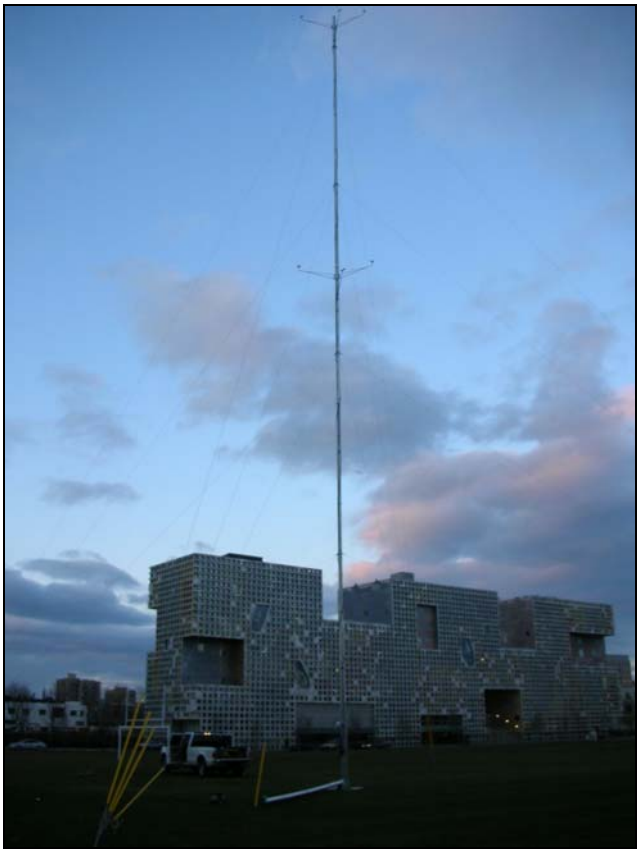

By the Wind Energy Projects in Action (WEPA) Full Breeze Project team:
Updated: November 27, 2010

Team Co-leaders:
Kathy Araujo, PhD Candidate, Urban Studies and Planning
Katherine Dykes, PhD Candidate, Engineering Systems

Resource Assessment:
Cy Chan, PhD Candidate, Computer Science
Katherine Dykes, PhD Candidate, Engineering Systems
Alex Kalmikov, PhD Candidate, Mechanical Engineering

Instrumentation and Integration:
Kevin Ferrigno, MS Candidate, Engineering Systems
Bryan Palmintier, PhD Candidate, Engineering Systems

Environment and Community Impacts:
Sungho Lee, PhD Candidate, Mechanical Engineering
Mark Lipson, PhD Candidate, Civil Engineering

Project Overview

The MIT Department of Facilities approached the wind energy sub-community in the spring of 2009 to assist in a study to aid the siting process for a potential small wind turbine on MIT's campus. Meetings were held in the spring and summer and it was determined that only a few sites on campus were possible for a ground-based small wind turbine. These included the open areas of Brigg's athletic fields as well as the green spaces near the Charles River. However, the space adjoining Memorial Drive and the Charles River fell on state-land and so the site consideration focused entirely on the athletic field. However, even within the field siting reflected a number of different concerns. Firstly, proximity to buildings posed a question due to 1) the negative potential impact on the communities using those spaces and 2) the positive benefit of being located near a structure where an electrical tie-in could be easily implemented. Secondly, use of the field by its current main stakeholder, MIT athletics, needed to be taken into account. Thirdly, the relative performance of the wind resource is an issue in a complex urban environment. Even over a small spatial distance, there can be substantial variation in the resource performance due to building and other structural interference. Given these concerns, a study that contrasted two potential sites was conducted. The two sites were chosen based on the criteria above with the first location near the west end of the field next to a parking lot and the second location near the east end of the field near the tennis bubble (see figure 1). The ability to install meteorological instrumentation at both sites and the use of advanced statistical and software modeling techniques allowed the characterization of the resource over the field to inform the site comparison. The use of visual "flicker" models allowed an assessment of the relative visual footprint of a potential turbine at each site and this was complemented by qualitative noise and environmental analyses to look at the overall community and environmental footprint. Finally, considerations of electrical interconnection and instrumentation were made in order to inform the overall relative feasibility of a small turbine at each of the two sites. The results of the resource, community and environmental analysis are provided in the subsequent sections of this report. The analysis on the electrical interconnection is part of the larger economic feasibility of the project and is beyond the scope of this document and study. The primary goal is to inform the decision process of MIT facilities along particular dimensions of interest rather than integrating all the pieces together for a particular recommendation of one site over the other.

Figure 1: Installation photos from MIT Project Full Breeze Sites 1 and 2

Table of Contents

List of figures and tables

List of Figures

List of tables

Analysis

A. *Resource Data Analysis and Energy Production*

Updated as of July 31, 2010

Cy Chan, PhD Candidate, Computer Science
Katherine Dykes, PhD Candidate, Engineering Systems
Alex Kalmikov, PhD Candidate, Mechanical Engineering

Resource assessment studies have been conducted at two locations on Brigg's field of MIT's campus. The two different test locations have been evaluated comparatively for the consideration of installing MIT's first campus wind turbine. On October 15, 2009, a set of meteorological measurement equipment, including 3 anemometers, 2 directional vanes and 1 temperature sensors, were installed on a light fixture located at (42° 21' 26.61" N, 71° 05' 53.01" W)[1]. The first site is located at the Northeast end of the field near the indoor-tennis structure. On December 15, 2009, a full 34 m NRG mini-meteorological tower was installed at (42° 21' 20.75" N, 71° 06' 06.78" W)[2] and included 4 anemometers, 2 directional vanes and 1 temperature sensor. This test site is at West end of the field in a relatively open area. Being located on an urban university campus, however, both towers were expected to be influenced by the complex effects of the surrounding built environment. Below are aerial images of the two sites on an aerial map.

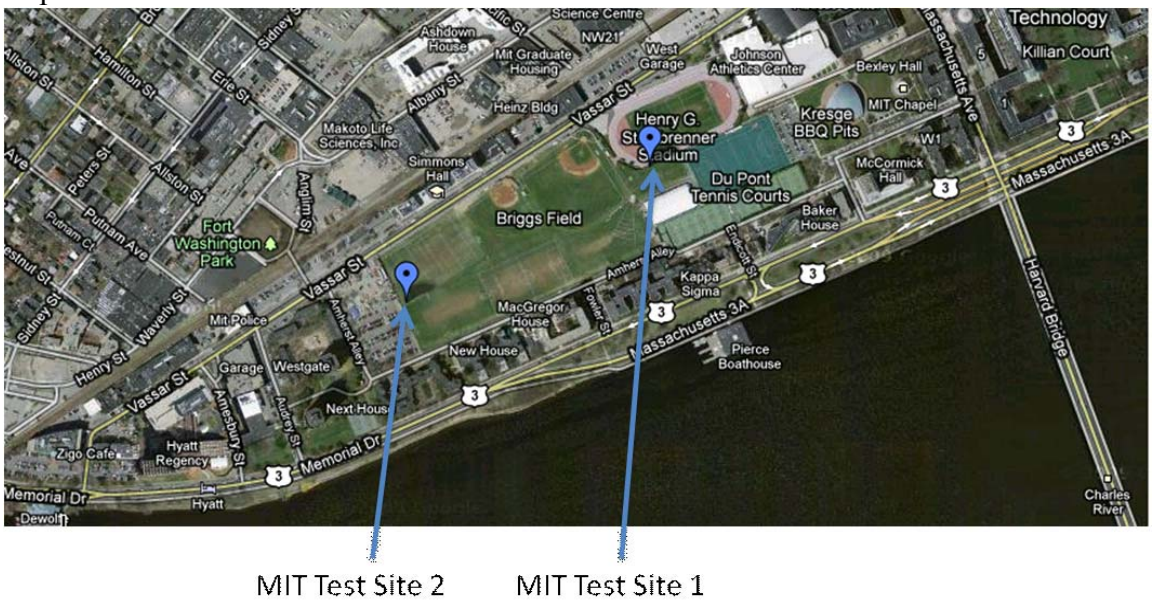

Figure 2: Aerial Image of Campus Test Sites

[1] Geographic coordinates: (Latitude, Longitude) = (42.357392, -71.098058) accuracy ± 2 meters.
[2] Geographic coordinates: (Latitude, Longitude) = (42.355765, -71.101883) accuracy ± 1 meter.

The proposed analysis for evaluating the sites with respect to each other involves statistics compiled from the filtered data, normalization of the data to long term trends, and simulation using advanced computer software analysis techniques such as computational fluid dynamics (CFD). So far, four months of data have been collected at test site 1 and two months of data have been collected at site 2. From this, the below preliminary analysis presents initial results of important summary statistics based on the data as well as normalization of the data and CFD analysis in order to study long term behavior of the two test sites.

Summary Statistics and Data Collection Overview

In order to produce the below statistics, the raw data collected went through a set of filtering steps and calculations. The data were collected at 2 second intervals for each sensor and then averaged over a 10 minute period. The NRG logger stored the average, standard deviation, maximum and minimum for each 10 minute period. Each week the data were inspected for potential sensor error issues. Each month, the data was processed through a filtering and calculation program. The data were filtered for different events such as icing, tower shadow, and sensor error. Monthly summary statistics for wind speed, direction, temperature were created and calculations for power density, turbulence intensity, and shear were made. Data retention after filtering was nearly 100% for all sensors of both test towers prior to filtering since neither icing nor sensor error were relevant during the collection period. The below table contains the summary statistics for the site as evaluated to date using a normalization routine.

Table 1a: Summary Statistics for site 1 based on both statistical and computational fluid dynamic analysis

	Met station 1					
Analysis Method	**MCP**	**CFD**	**MCP**	**CFD**	**MCP**	**CFD**
Height [m]	20	20	26	26	34	34
Mean Wind Speed [m/s]	3.3	2.7	3.7	2.9	n/a	3.1
Power Density [W/m^2]	39.4	41.9	55.6	50.2	n/a	60.5
Annual Energy Output [kW-hr]	817	974	1,259	1,193	n/a	1,430
Annual Production CFD [kW-hr]	n/a	931	n/a	1,135	n/a	1,377
Capacity Factor	4%	5%	6%	6%	n/a	7%
Operational Time	35%	26%	45%	29%	n/a	32%

Table 2b: Summary Statistics for site 2 based on both statistical and computational fluid dynamic analysis

	Met station 2					
Analysis Method	**MCP**	**CFD**	**MCP**	**CFD**	**MCP**	**CFD**
Height [m]	20	20	26	26	34	34
Mean Wind Speed [m/s]	3.4	2.9	n/a	3.0	4.0	3.2
Power Density [W/m^2]	46.5	51.7	n/a	60.4	74.6	70.9
Annual Energy Output [kW-hr]	1,017	1,185	n/a	1,384	1,791	1,609
Annual Production CFD [kW-hr]	n/a	1,136	n/a	1,328	n/a	1,558
Capacity Factor	5%	6%	n/a	7%	9%	8%
Operational Time	38%	28%	n/a	30%	51%	33%

From the above summary characteristics, it can be seen that either through the statistical or fluid dynamic analysis methods, site 2 slightly outperforms site 1. The difference can mean a slight difference in terms of expected output as well as operational time. In siting an urban wind turbine, operational time is important since this affects how the public will perceive the machine. If it is operating only a small percentage of the time, it will not be perceived as an effective installation even if it is cost-effective. However, the resource and expected output are just one of the factors that affect siting and must be taken in context. The difference between the two sites is small enough such that many other issues such as installation costs, aesthetics and public perception, etc may outweigh the small difference.

Returning to the wind resource, many factors can contribute to site-specific average wind speed characteristics. These may include topography as well as both manmade and natural obstructions. According to wind maps of 2.5 km resolution, the prevailing wind direction around the MIT campus comes from the south-southwest. However, direct measurements during the winter season clearly demonstrated prevalence of the north-westerly winds (see discussion in Physical Analysis section). The test sites at MIT are surrounded on all sides by a large number of obstructions (i.e. the campus built environment) as shown in the aerial view of Figure 1. As can be seen in the photo, there are a large number of buildings surrounding the site. All of these structures can provide sources of interference to wind flow reducing the wind speeds and increasing the levels of turbulence intensity. As will be shown in subsequent sections, analysis reveals several indications that obstructions nearby the site may be influencing test results. These include the wind shear (or vertical differences in wind speeds), the level of turbulence intensity in the wind speed data and the uniformity of the wind direction frequency distribution. All of these factors were affected at the measurement heights of interest for

turbine installation. The next sections discuss in more detail each of the summary statistics for the site as shown in table 1 as well as provide an analysis to characterize long term behavior of the two locations.

Wind Speed

Monthly Averages

The following plot gives the site measured monthly average wind speeds and diurnal average wind speeds. For met tower 1, thee anemometers were placed at 15, 20 and 26.5 m heights. For met tower 2, four anemometers were placed at two heights of 21 and 34 m heights. The resulting wind speed average for each 10 minute average were filtered for tower shadow and then averaged together in order to create a wind speed average for each height. Monthly averages were then created from the data set and are represented graphically below. Only a half month of data is available for October 2009 and March 2010 for met tower 1 as well as for December 2009 and March 2010 for met tower 2. The difference in average wind speeds between subsequent levels is about 0.1 to 0.5 m/s for each month indicating a substantial amount of wind shear (or vertical difference in wind speed) at the sites up to and extrapolated beyond 26 and 34 m respectively for test towers 1 and 2. From the limited set of data collected thus far, it appears that test site 2 has stronger wind speeds than site 1. The 20 m averages for site 2 are similar to the 26 m averages at site 1 which are both substantially lower than the 34 m averages at site 2. This is despite the fact that the towers are so near to each other and demonstrates how important such a study as this can be in terms of siting wind turbines in urban and complex terrain environments.

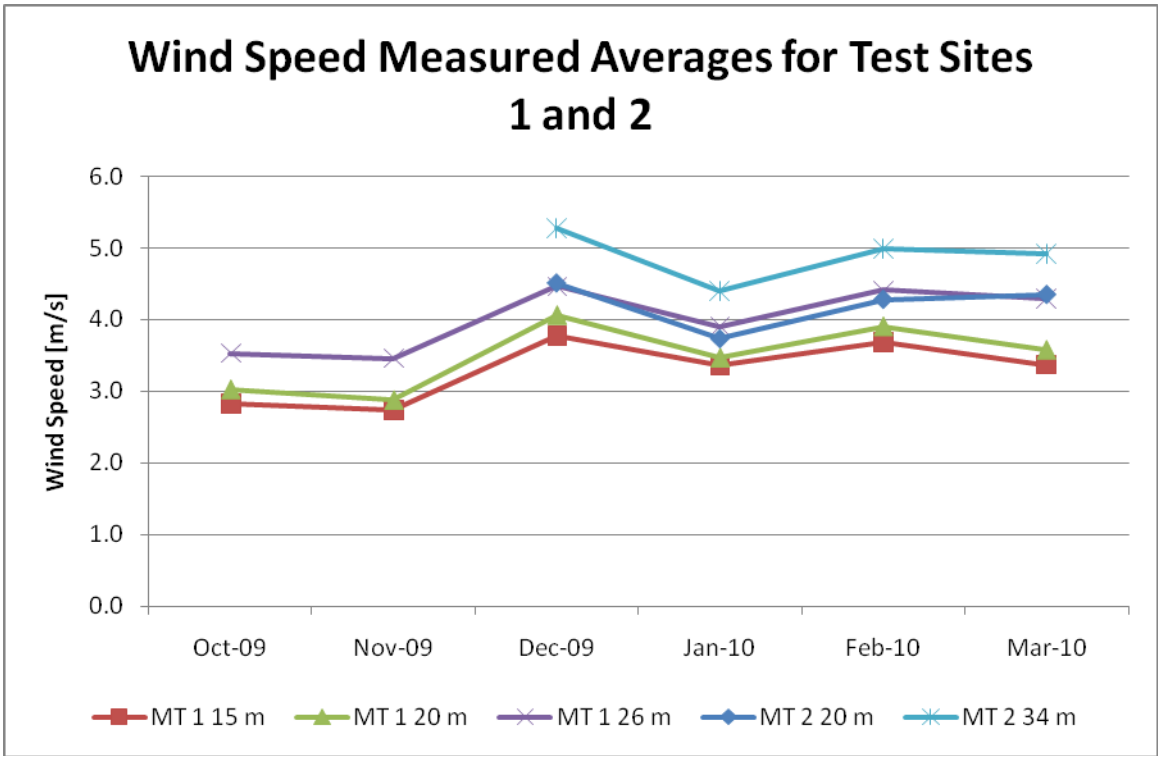

Figure 3: Monthly Average Wind Speeds for all Measured Heights

Diurnal Averages

The diurnal plot shows wind speed averages for the year on an hourly basis. The plot below shows that over the last few winter months, wind speeds are slightly higher mid-day than they are at night or in early morning. Given that electricity demand is generally strongest during the day, this implies that there is some potential for diurnal matching of wind power output and electricity demand. However, this data set represents only a few winter months of data and the diurnal pattern is typically dependent on seasonal variations in the local wind profile.

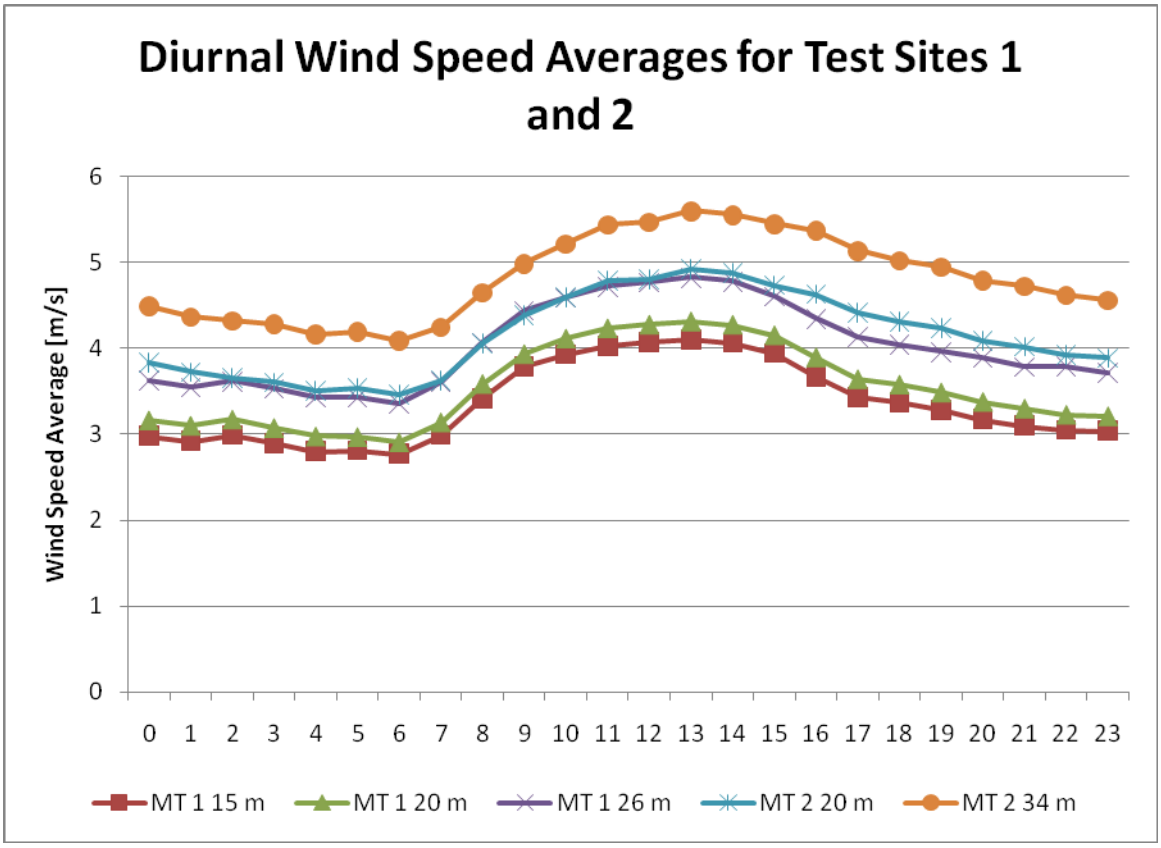

Figure 4: Diurnal Wind Speed Averages for all Heights

Frequency Distribution

In addition to the monthly averages, a histogram, or frequency distribution, of wind speeds provides more insight into the wind behavior at the site for power production by showing the amount of time the site is expected to be within a given 0.5 m/s wind speed range during the course of the year. This gives an indication of how much of the time a wind turbine at the site might be operational and when coupled to a turbine power curve (as discussed in a later section) will give estimate of potential power output for a specific site-turbine combination. The histogram also gives information about the highest sustained wind speeds that can be expected (as obtained from the 10 minute averages). That is, the highest wind speeds a turbine would need to withstand during operation during the study year were about 12 m/s for only a handful of occurrences. This

information, however, does not represent the highest instantaneous gust of wind that the turbine might experience. The gusts as measured at each test site were less than 23 m/s. Other notable features of the frequency distribution plot is the shift right in the distributions moving from lower to higher heights which represents increasing with height. The site shows wind speeds characteristic of a Weibull distribution as is typical for sites where wind resource assessments are performed. Between sites 1 and 2 there is a gradual shift to the right meaning that not only the average wind speeds for site 2 are higher but also that wind speeds are higher for a larger portion of the overall year at this test site. This implies that a turbine installed at site 2 during the data collection period would have likely been in operation more of the time than one installed at site 1. However, in order to compare the long term expected behavior of the two sites, the data must first be normalized and extrapolated to an annual data set. Please see the section on *Normalization* for more details.

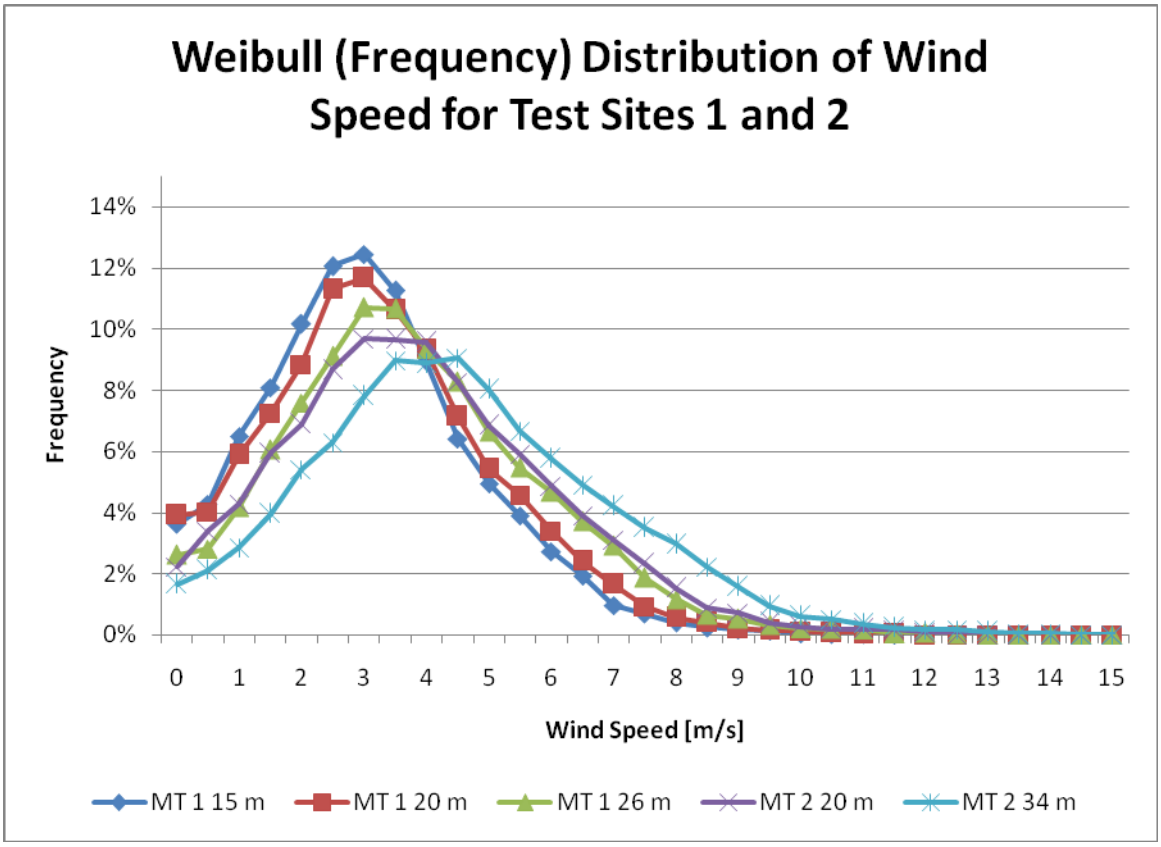

Figure 5: Wind Speed Frequency Distributions for All Heights

Wind Shear Monthly Averages

Wind shear values shown in the plot below varied considerably by month and for the different height separations of 15 to 20, 20 to 26 and 20 to 34 m. Wind shear is a measure of the relationship between height and wind speed. This can be helpful in determining optimal hub height for turbines at a given site. The wind shear equation is given by:

$$V = V_0 \left(\frac{z}{z_0}\right)^{\alpha}$$

Here V is the wind velocity and z is the height. The subscript "o" indicates a reference height. The coefficient α is called the wind shear exponent. Normally it takes a value of approximately 0.143 for clear, topographically level land.[3] The average value of wind shear, α, calculated for the two test site varies between 0.10 and 0.50 with averages around 0.30. Such high values are again indicative of the influence of surrounding obstructions on the site measurements. The wind speeds at each height are likely impacted by the surrounding obstructions and the shear values could increase even further for higher heights. However, wind shear is not constant with increasing height and will typically be less between higher heights (near potential hub levels) as compared to the lower heights (used for measurements) so extrapolations as presented in later sections should be treated lightly as estimates of potential turbine behavior at those heights. Also, it is important to not overlook the amount of variation in month to month wind shear exponent values for each test site. This is again indicative of the complexity of the wind profile at this urban site.

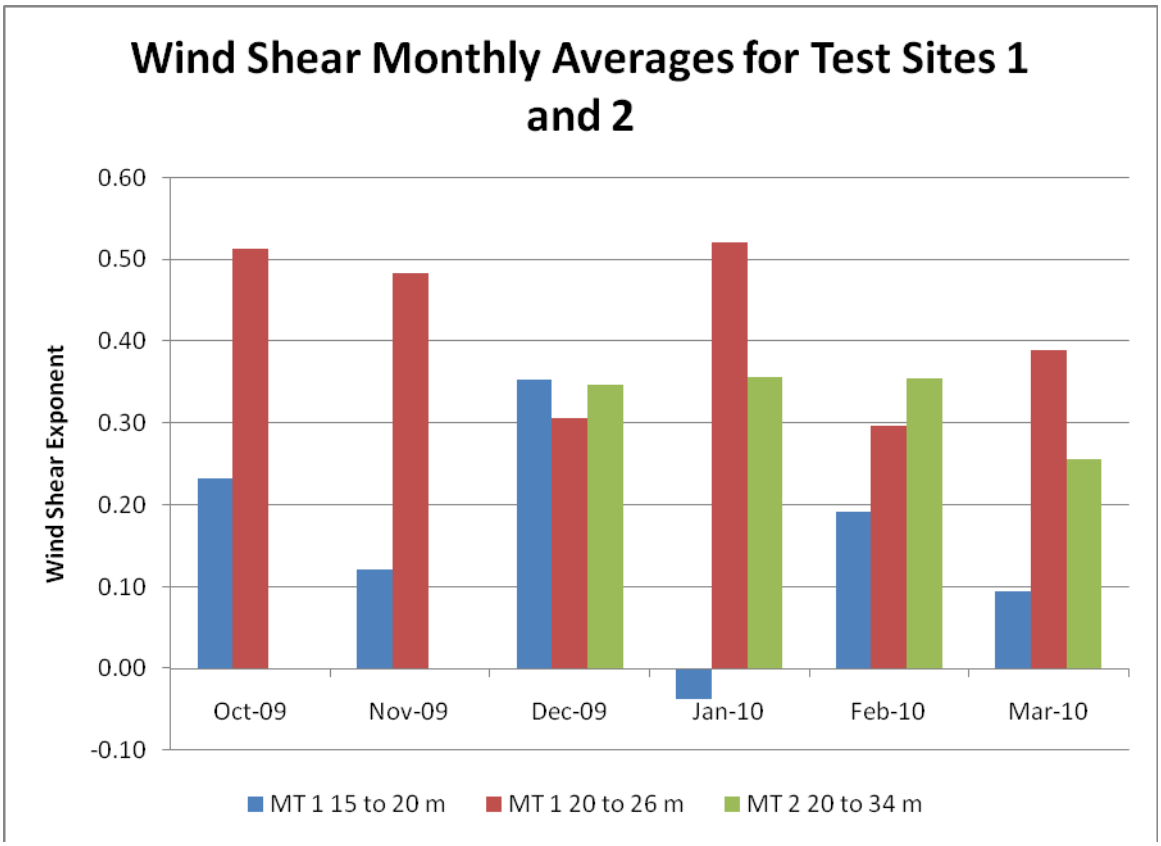

Figure 6: Wind Shear Monthly Averages [Dimensionless]

Turbulence Intensity

Turbulence intensity is a measure of how intermittent the air flows at the test site. The value is calculated by taking the standard deviation of the wind speed and dividing them by the mean values of wind speed. Turbulence intensity averages for the site are

[3] *Wind Resource Assessment Handbook: Fundamentals for Conducting a Successful Wind Monitoring Program*, AWS Scientific, Inc., April 1997.

relatively high at around 0.25 to 0.35 when compared to the values one would expect for clear and flat land (approximately 0.143). This is again indicative of the fact that manmade and natural obstructions do likely have a significant impact on wind speed measurements at the site. Advanced software analysis using computational fluid dynamic models will likely provide more insight into the influence of the complex terrain on these characteristics of wind speed, turbulence intensity and shear.

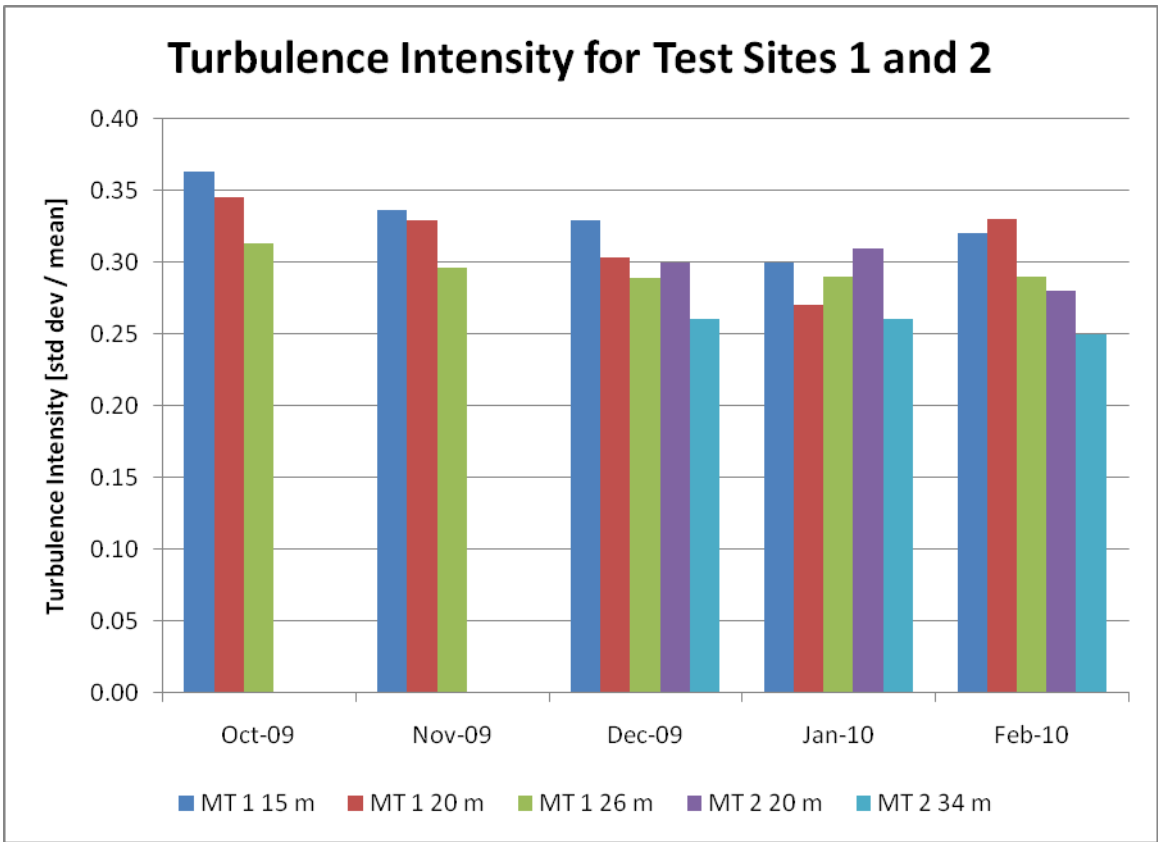

Figure 7: Turbulent Intensity Monthly Averages for All Heights

Temperature

The plot shown below gives monthly average temperature for the site. Air density, which directly impacts power density, is affected by temperature such that higher temperatures result in lower air density (gas expansion versus compression) so that air density is higher in the winter months. Temperature coupled with higher wind speeds in general mean that power density is typically much higher in the winter months. The large difference in temperature in December is indicative of the fact that only half a month of data is available for MIT Test Site 2 during that month. The discrepancy in temperature for January and February require further inspection to determine whether there is a potential sensor issue or some effect of the local surroundings (i.e. differential shadowing of the sites during the day from the surrounding buildings).

Monthly Average Temperature

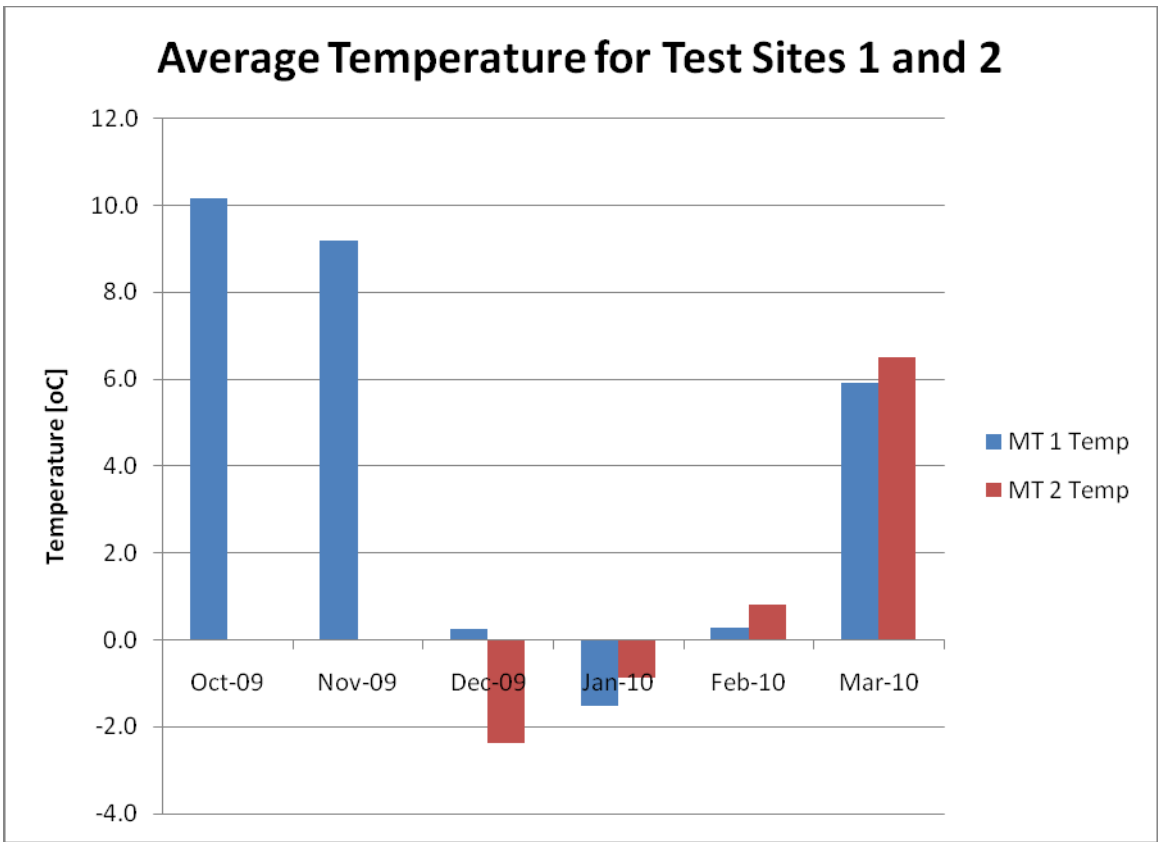

Figure 8: Monthly Average Temperature at Site (Logger Height)

Power Density

The combination of information on wind speed and temperature allow for the calculation of power density at the site for a given height. Power density describes the maximum amount of power contained in the wind per square meter of area. The interaction of the turbine and power density determines the actual power output for the site. In general, the maximum amount of power that can be extracted from the wind is 59% as given by the Betz limit for a horizontal flow through an ideal rotor cross section.[4] Thus, an ideal turbine would extract 59% of the power density as shown below for the site but due to deviations from ideal in terms of finite blades as well as mechanical and electrical losses, the actual efficiency of a turbine will actually be lower. In addition, turbines are optimized for operation between a certain ranges of wind speeds such that for much of the year, they are not operating in an ideal state further reducing overall efficiency. Thus, power density can be thought of as an idealized representation of power production by a wind turbine. The general equation used to calculate power density is:

$$power\ density = PD = \frac{1}{2}\rho V^3$$

[4] Betz, A. "Wind Energy and its Exploitation by Windmills." Vanderhoeck and Ruprecht, Gottingen, Germany, 1926.

Here ρ is the air density, and V is the wind velocity. Thus, power density results from a cubed function of wind speed where a doubling of wind speed leads to 8 times the power contained in a given body of wind. In addition, air density varies with pressure, temperature and elevation. For the power density calculations, air density was calculated dynamically as a function of the temperature and elevation of the site:

$$\rho = \left(\frac{358}{273 + Temperature}\right) * e^{\left(\frac{-0.034 * (elevation + channel\ height)}{273 + Temperature}\right)}$$

Here, temperature is the site temperature in Celsius, elevation is the site elevation in meters, channel height is the height in meters above ground of the anemometer in question, and is the air density in kg/m3. Monthly average power density for the site at each height is shown in the below plot. Notice that the power density for test site 2 at 34 m is significantly more than the rest of the locations again due to the fact of power dependency on the cube of wind speed.

Monthly Averages

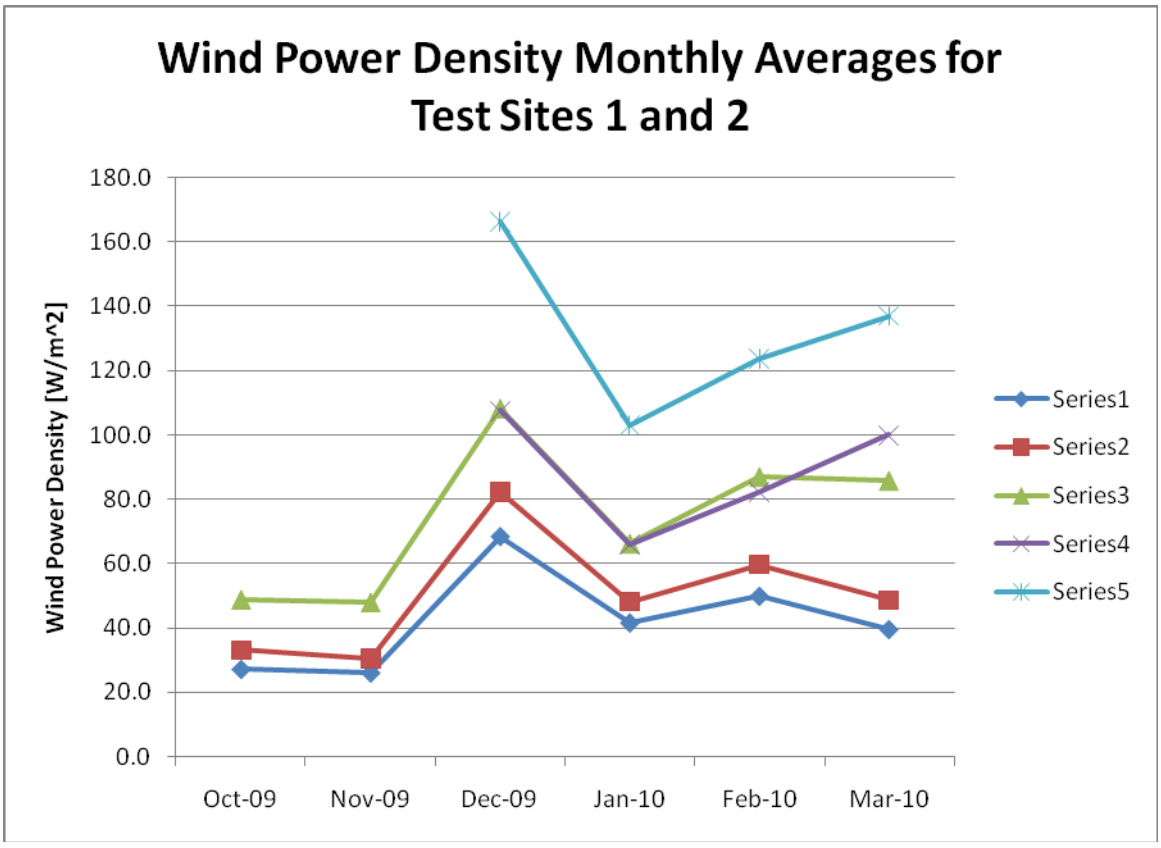

Figure 9: Monthly Average Power Density for All Heights

Wind Direction

Frequency Radar Plot

In siting a turbine, dominant wind direction becomes important in optimizing turbine location in terms of proximity to obstructions as well as relative to other turbines in a

wind farm configuration. The below radar plot of wind direction frequency indicates that the predominate wind directions at the site is from the west. The complex terrain and urban built environment is likely having an impact on the specific wind direction characteristics of the two test sites. Comparison to regional plots will show how the test site wind roses differ substantially from the regional trends. More detail of this will be discussed in the following sections on *Physical Wind Resource Assessment*.

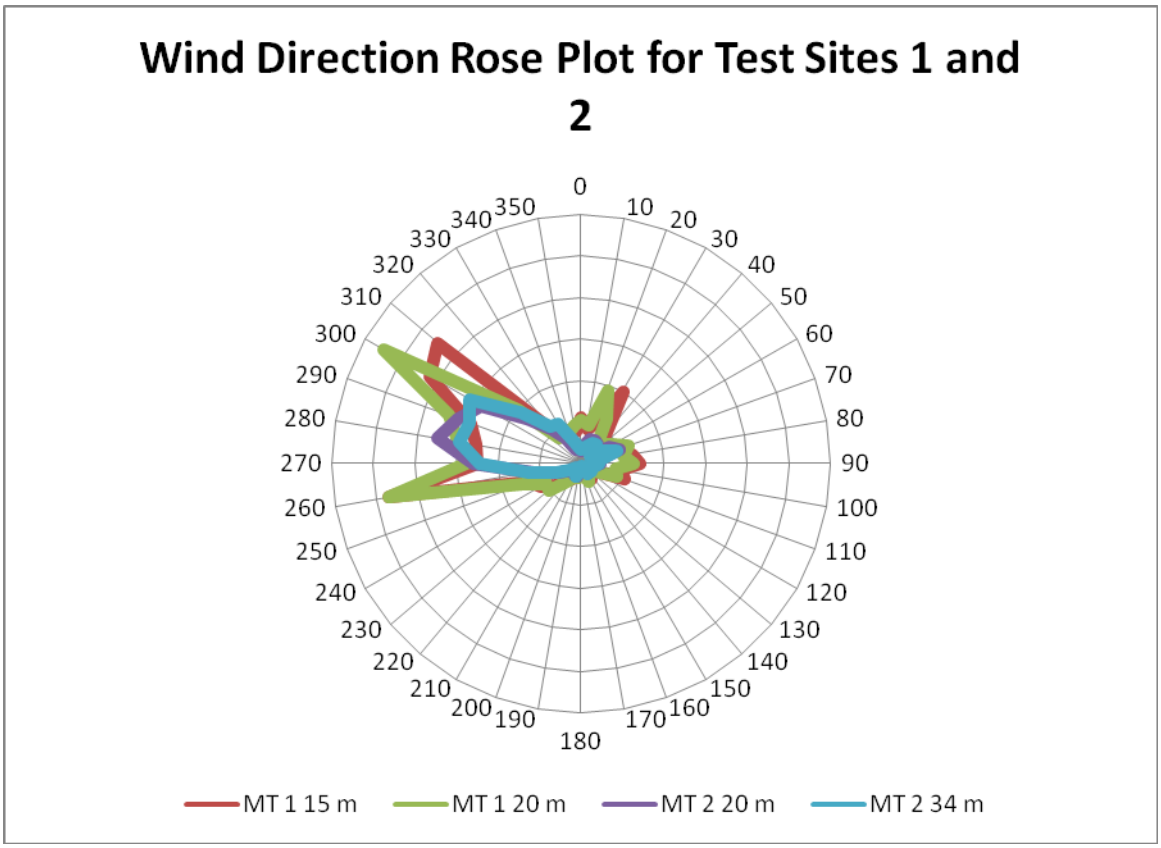

Figure 10: Wind Direction Frequency Plot for MIT Test Sites 1 and 2

Normalization

Normalization of the collected wind data is necessary to estimate the seasonal behavior of the wind resource over the course of the full year. We used long-term data obtained from the NCDC Quality Controlled Local Climatological Dataset (QCLCD) for Boston's Logan Airport to do a Measure-Correlate-Predict (MCP) analysis. To generate our monthly statistics, we used synthesized 10-minute averages computed by interpolating the QCLCD Logan dataset over the years 1997 through 2009. The seasonal variability of the wind resource at Logan is shown in Figure 10, which shows how the Weibull scale and shape parameters vary according to the month of the year.

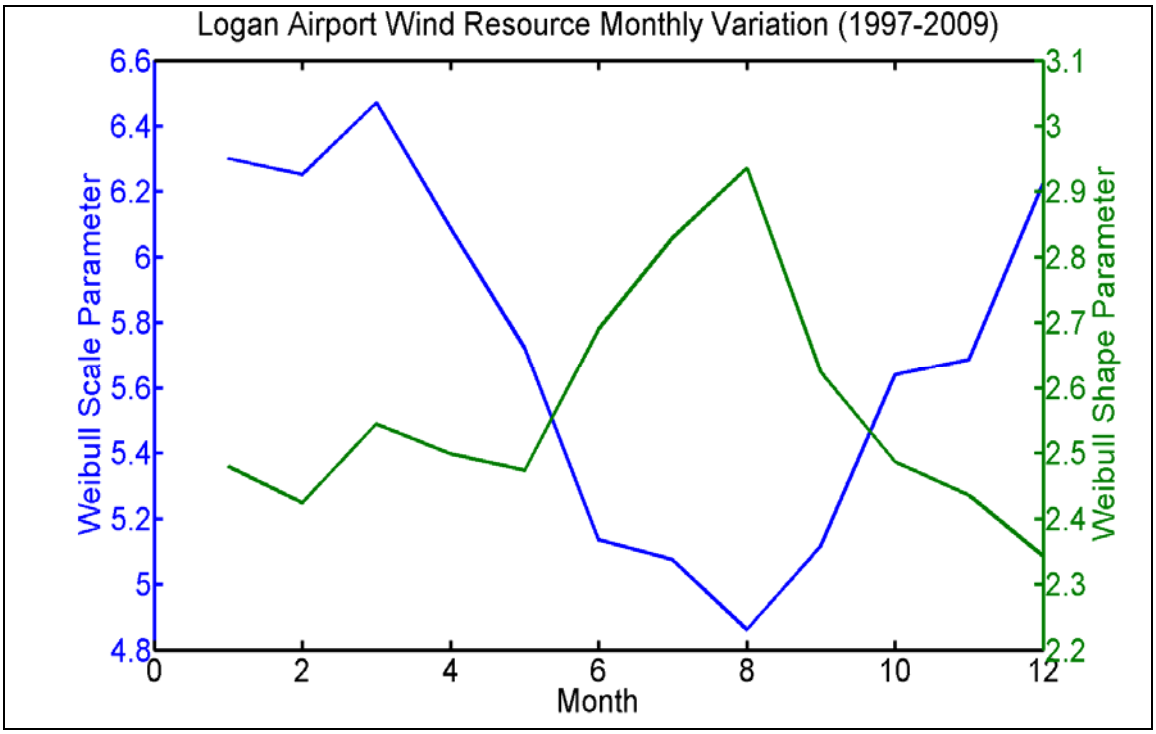

Figure 11: Seasonal Variation of the Logan Airport Weibull Distribution parameters

For the time period over which our data were collected, wind speeds and directions are very well correlated between our met towers and Logan's data. Over all of our locations and heights, correlations with Logan varied in the narrow range of 0.84 to 0.86 for wind speeds and 0.96 to 0.97 for wind directions[5]. For example, the below figures show the wind speed and direction, respectively, for Met Tower 2 at 34m height plotted versus Logan.

To estimate the distribution of wind speeds at the target locations, we used a binned linear regression based MCP method. Each sample point in our training set was binned according to the wind direction at Logan. We used bins of size 30 degrees each centered at {0, 30, 60, … , 330}. A separate set of linear regression coefficients (slope and intercept) was determined for each of the bins. For each data point in the Logan dataset, we computed an estimated wind speed at the test site using the regression coefficients corresponding to the wind direction at Logan. Since the linear regression underestimates the variability of the wind resource at the test site, we added Gaussian noise with a standard deviation equal to the residual standard deviation observed during regression analysis. This method yields more accurate estimates of statistics such as the Weibull shape parameters and power density estimates at the test site.

[5] The wind direction correlation coefficients were computed by wrapping the measured met tower wind directions around (by adding or subtracting 360 degrees) such that the differences between them and the Logan vane are between -180 and +180 degrees. This was done to prevent situations like 0 and 359 degrees appearing to be very far apart when they are actually only 1 degree apart. See Figure 12 for a graphical demonstration of this. More scatter can be seen for MT1 then MT2 in this graphical representation.

Using this methodology, we obtained the estimated seasonal mean wind speeds and power densities given in this section. The estimated seasonal Weibull scale and shape parameters are given as well.

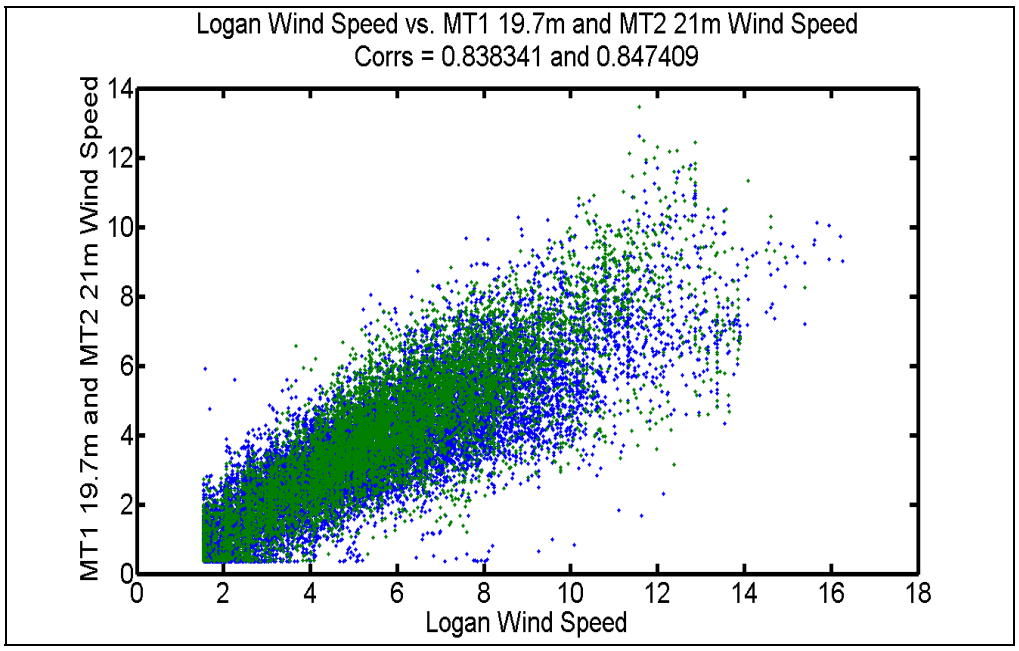

Figure 12: Observed correlation between Logan Wind Speed and Met Tower 1 19.7m (blue) and Met Tower 2 21m (green) Wind Speeds

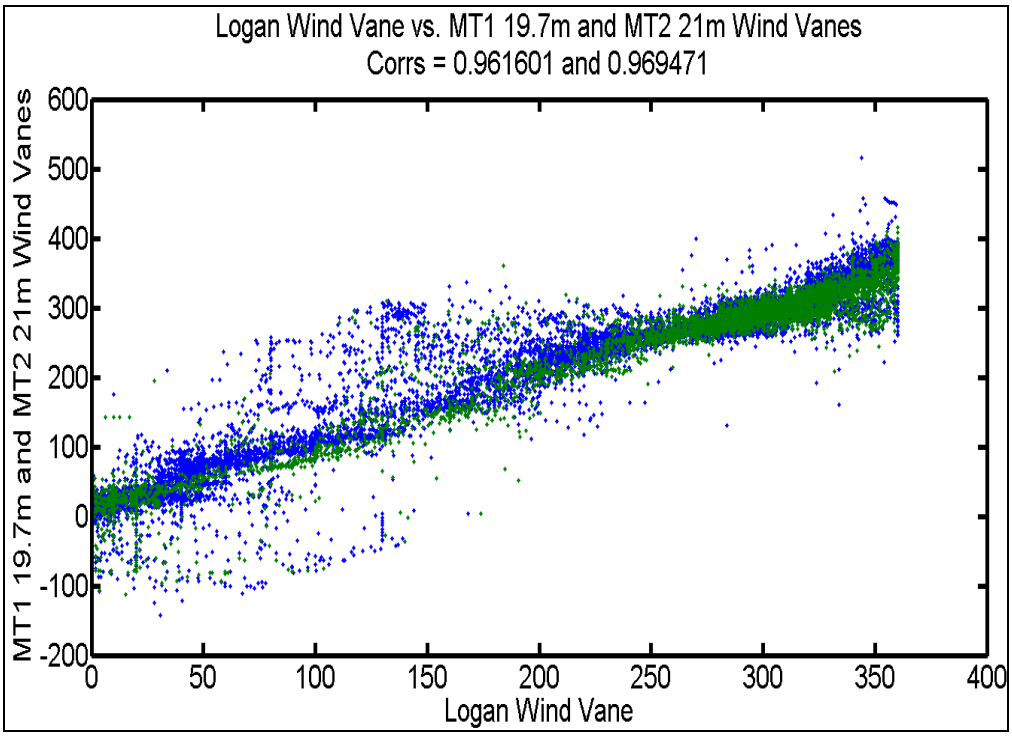

Figure 13: Observed correlation between Logan Wind Vane and Met Tower 1 19.7m (blue) and Met Tower 2 21m (green) Wind Vanes

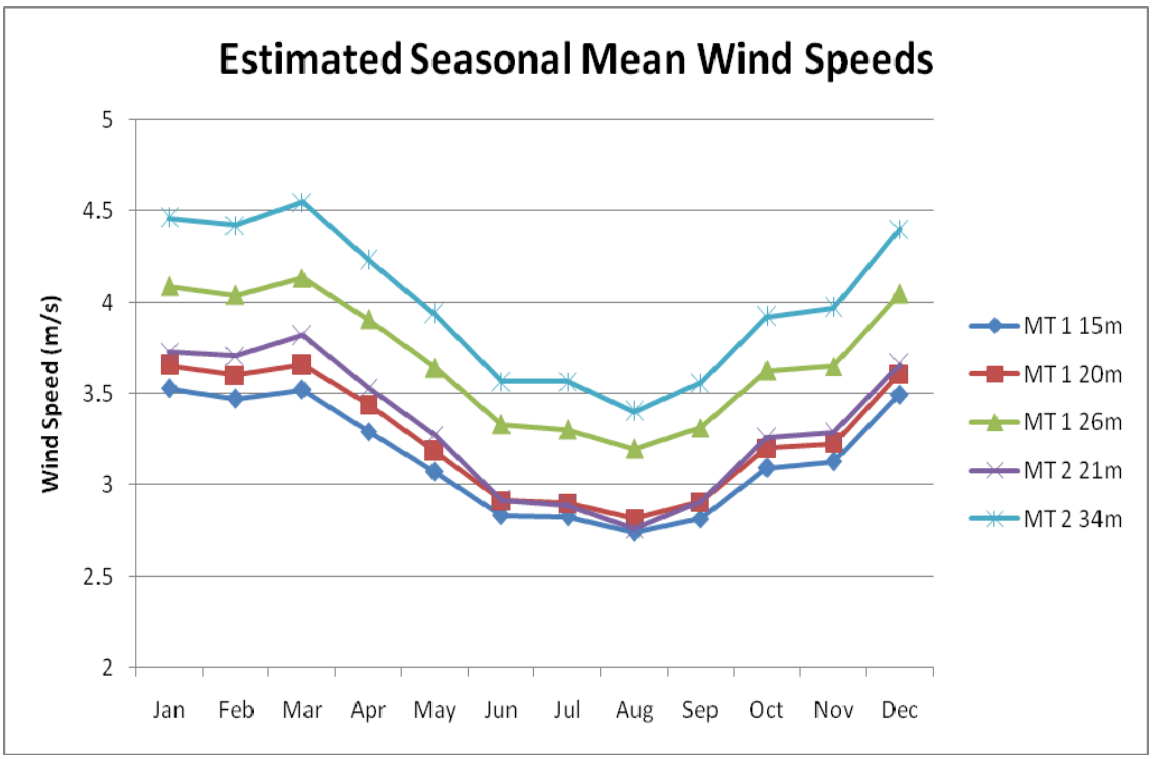

Figure 14: Estimated Seasonal Mean Wind Speeds

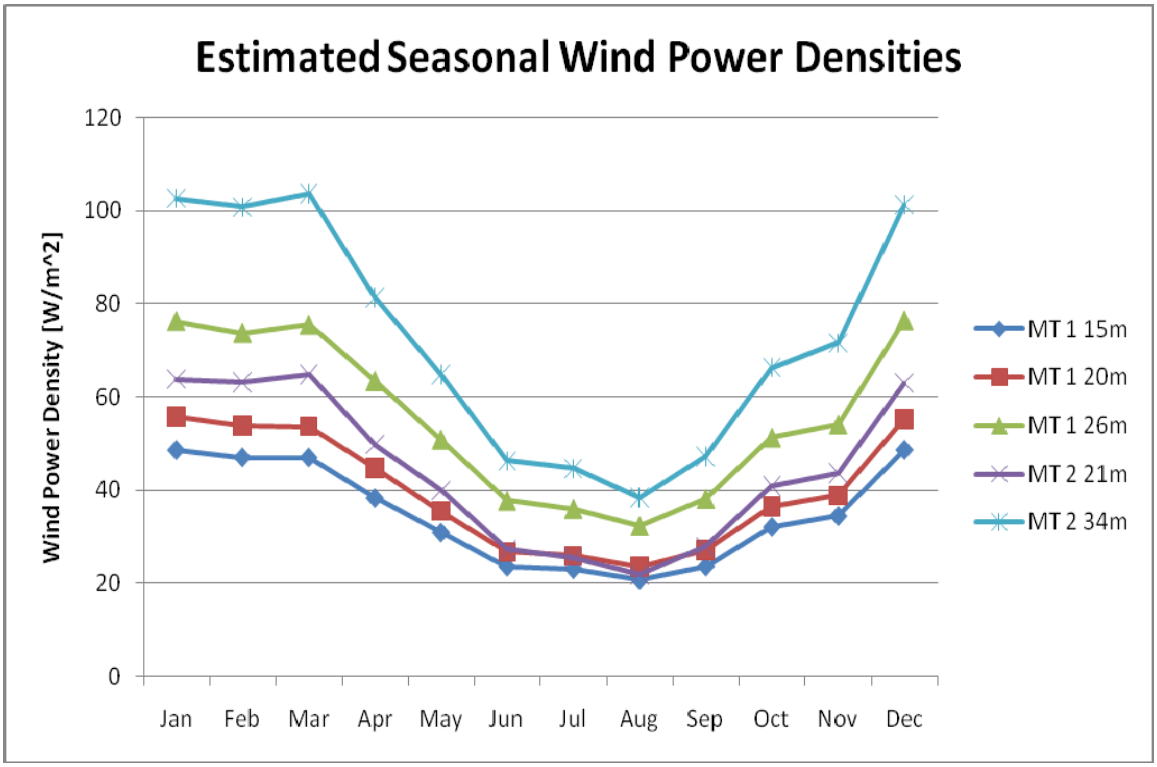

Figure 15: Estimated Seasonal Wind Power Densities

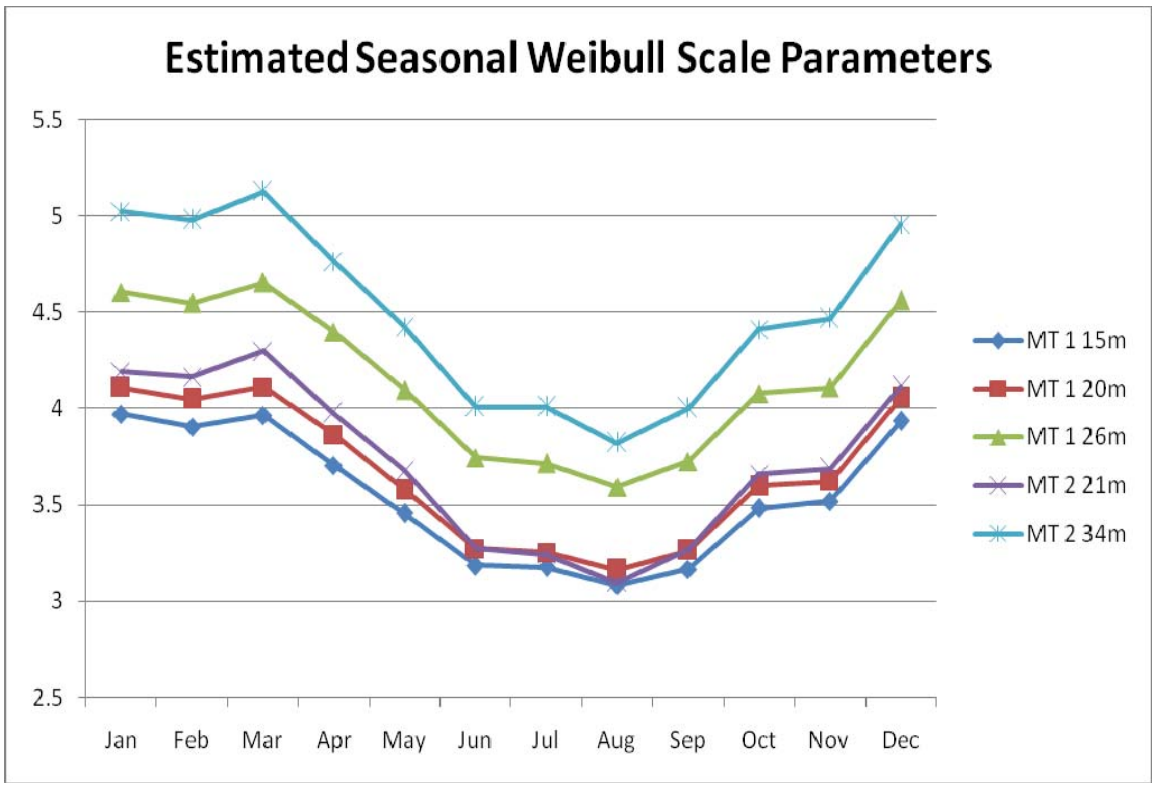

Figure 16: Estimated Seasonal Weibull Scale Parameters

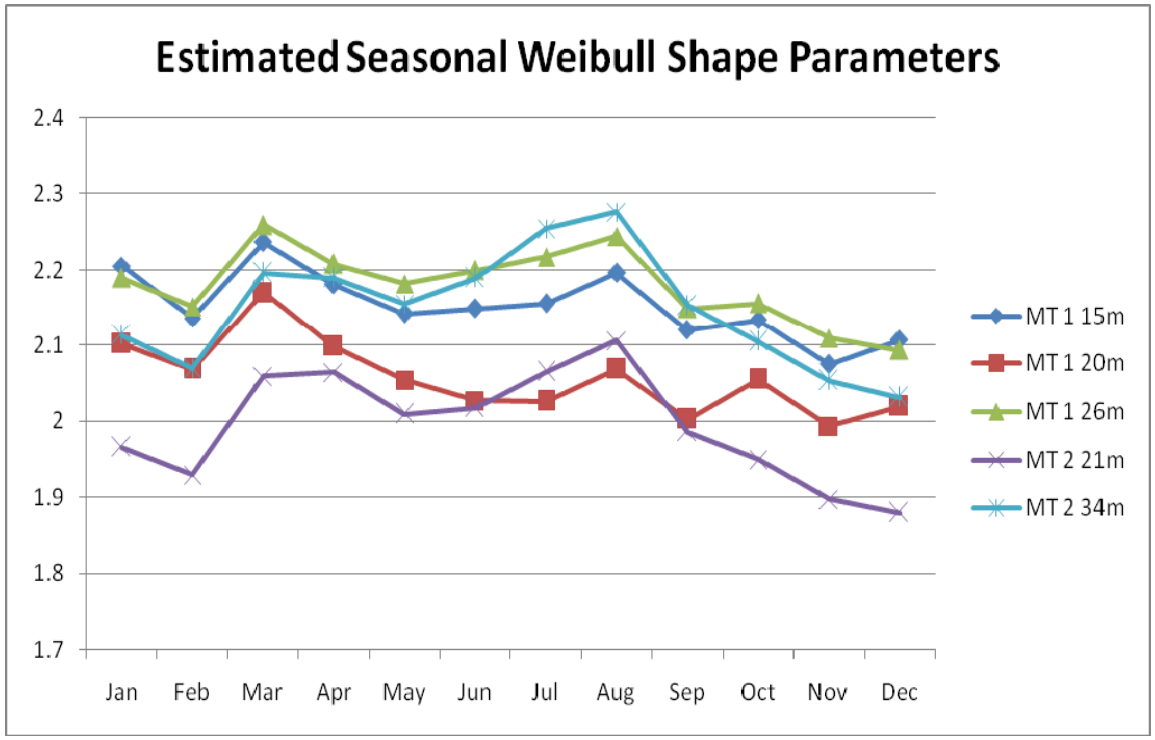

Figure 17: Estimated Seasonal Weibull Shape Parameters

In the above figures, it can be seen that the measured wind power density at MT 2 at a height of 21 m is similar to that at MT 1 at a height of 26 m. At first glance, this would

seem to indicate that the wind resource at MT 2 is better than that at MT 1. However, the estimated seasonal wind power densities given in Figure 14 indicate that those two location/heights should differ by about 10 W/m^2 on average. We believe that there are two major reasons for this discrepancy.

First, these figures use all available data when computing the mean wind power density for a particular month. Data was available for MT 1 for the entire month of December, while for MT 2 data was only available for the second half of December. Figure 17 shows measured wind power densities with the second half of December separated so we may compare the available MT 2 data with only the corresponding MT 1 data from the same time frame. In the new figure, we see that MT 1 - 26 m yields an average of 13 W/m^2 greater power density than MT 2 - 21 m in the second half of December.

Since the estimated seasonal statistics are trained using data from mid-December through mid-February, and the measured wind resource at MT 1 - 26 m was measurably better than that at MT 2 - 21 m during the December and February half-months, this accounts for a large part of the difference seen in the resulting regression estimates. In other words, the regression predicts a better resource at MT 1 - 26 m because the wind was measurably faster during the shoulder months of the training period. This was the first cause for the divergence of the two sites in the estimates.

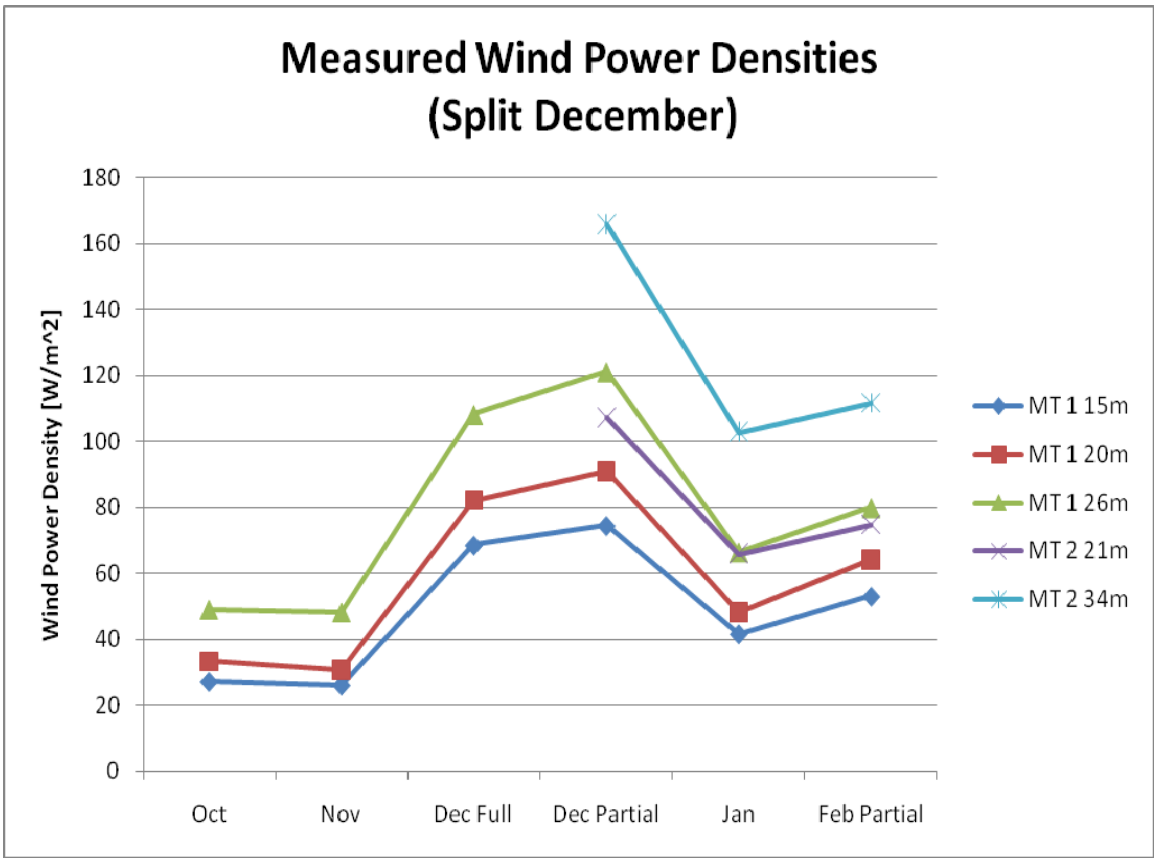

Figure 18: Measured Wind Power Densities with December split between Full and Partial months

Second, the direction of the wind during the month of January was more northwesterly than usual. Figure 18 shows a histogram of wind samples collected at Logan by wind vane direction for both the training period (blue) and the average January trend measured over 1997-2009 (green). The figure shows that the training period saw more frequent winds from the northwest and less frequent winds from the southwest than typically seen in a Boston January.

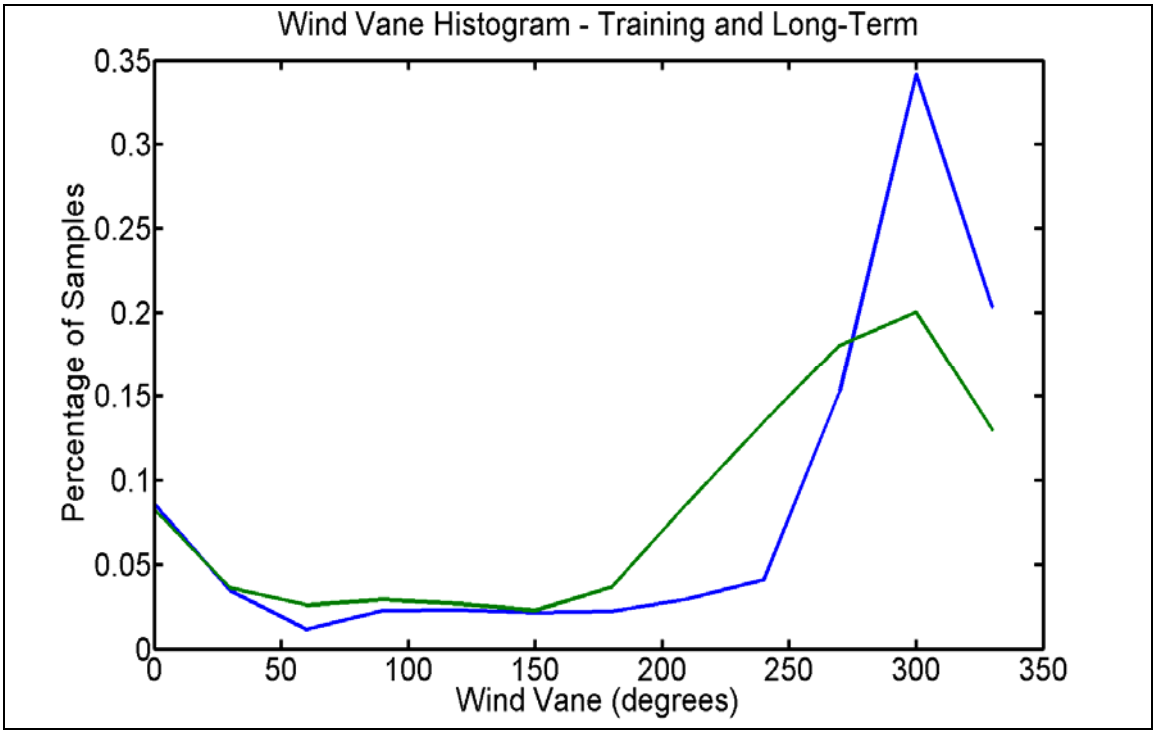

Figure 19: Wind Vane Histogram – Training Period (blue) and January Long-Term averages (green)

The figure above shows the regression coefficients solved for during the training period for both MT 1 – 26 m (blue) and MT 2 – 21 m (green). The significant point of this figure is that by trading some of the abnormal northwesterly winds for southwesterly winds to get a statistically representative month, the MT 1 – 26 m responds with slightly higher wind speeds, while MT 2 – 21 m responds with slightly lower wind speeds.

It is important to note that since we have limited training data, it is unclear whether this observed behavior generalizes well in the long-term, especially since the regression coefficient graph appears to be noisy. However, this second effect was only a partial contributor for the observed divergence between the two sites in the seasonal estimates. The first cause explained earlier is based on the observation of stronger winds at MT 1 – 26m than MT 2 – 21m during the shoulder months of the training period. Taken together, these two mechanisms present plausible justification for the divergence between the two anemometer locations in the estimated seasonal statistics. Hence, we should not conclude that MT 2 is a stronger candidate for placement of the turbine than MT 1 based on the raw data alone.

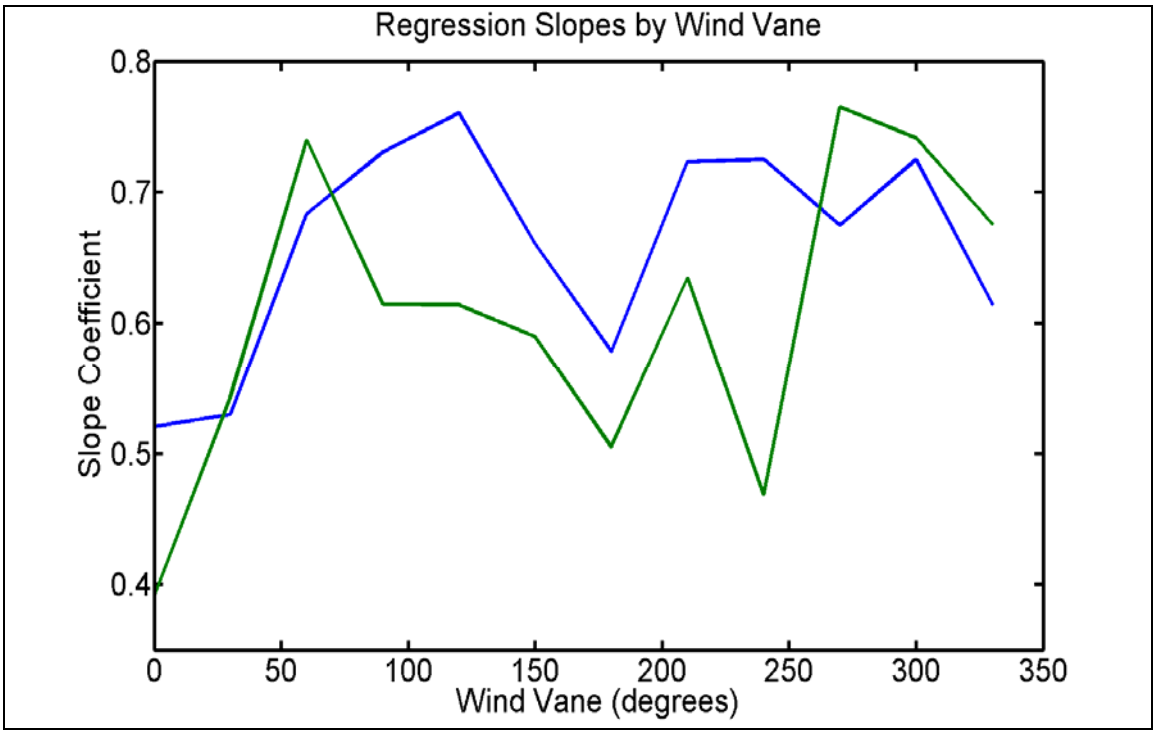

Figure 20: Regression Slope Coefficients by Wind Vane Direction: MT 1 – 26 m (blue) and MT 2 – 21 m (green)

CFD modeling

Wind flow in the complex urban geometry of the campus was simulated with a CFD model in order to enhance the traditional observation based resource assessment by extending the spatial coverage of the localized estimates and by providing a physical insight on the governing flow mechanisms to explain the variability of wind resource due to the complex geometry. The resource assessment was enhanced by integration of local wind measurements and observations from nearby reference sites into the CFD model in order to estimate the local long-term climatology. Measurements from the two site specific met masts and their climatological normalizations were compared to the simulated results, which allowed validation of the modeling for mean wind speed, wind power density and wind variability parameterized by Weibull distribution. CFD analysis provides an improved understanding of the micro-climate of wind resource on the MIT campus and facilitates the optimal siting of the turbine.

The three dimensional model of campus geometry was generated based on the GIS data from City of Cambridge GIS. The data was downloaded from the MIT Geodata Repository – the GeoWeb[6] and analyzed with ArcGIS software suit (Figure 20). The three dimensional wind flow fields were modeled with a "Virtual Wind Tunnel" methodology: essentially simulating the standard experimental practice of placing a scaled model of building geometry in a wind tunnel. The wind is assumed to blow from a predetermined inlet direction and exits the experimental area from the opposite side, while the scaled down three dimensional model of the buildings is rotated with different angles to the inflow direction.

The hydrodynamic simulations were implemented with a commercial CFD model ***Urba****Wind* by Meteodyn. The model solves Reynolds Averaged Navier-Stokes equations (RANS) for steady incompressible flow, parameterizing the subgrid turbulence in K-L framework. The model automatically generates boundary conditions, applying symmetry condition at the lateral boundaries, a reflecting condition at the upper boundary and a homogeneous pressure condition at the outlet. The mesh is automatically generated for each computed direction aligned with the inflow (Figure 21). For further details on the CFD modeling see Kalmikov et al. 2010[7].

---

[6] http://web.mit.edu/geoweb/

[7] Kalmikov A., G. Dupont, K. Dykes and C. Chan, 2010: Wind resource assessment in complex urban environments: MIT campus case-study using CFD Analysis. *Proceedings of AWEA Windpower Conference 2010, Dallas TX.*

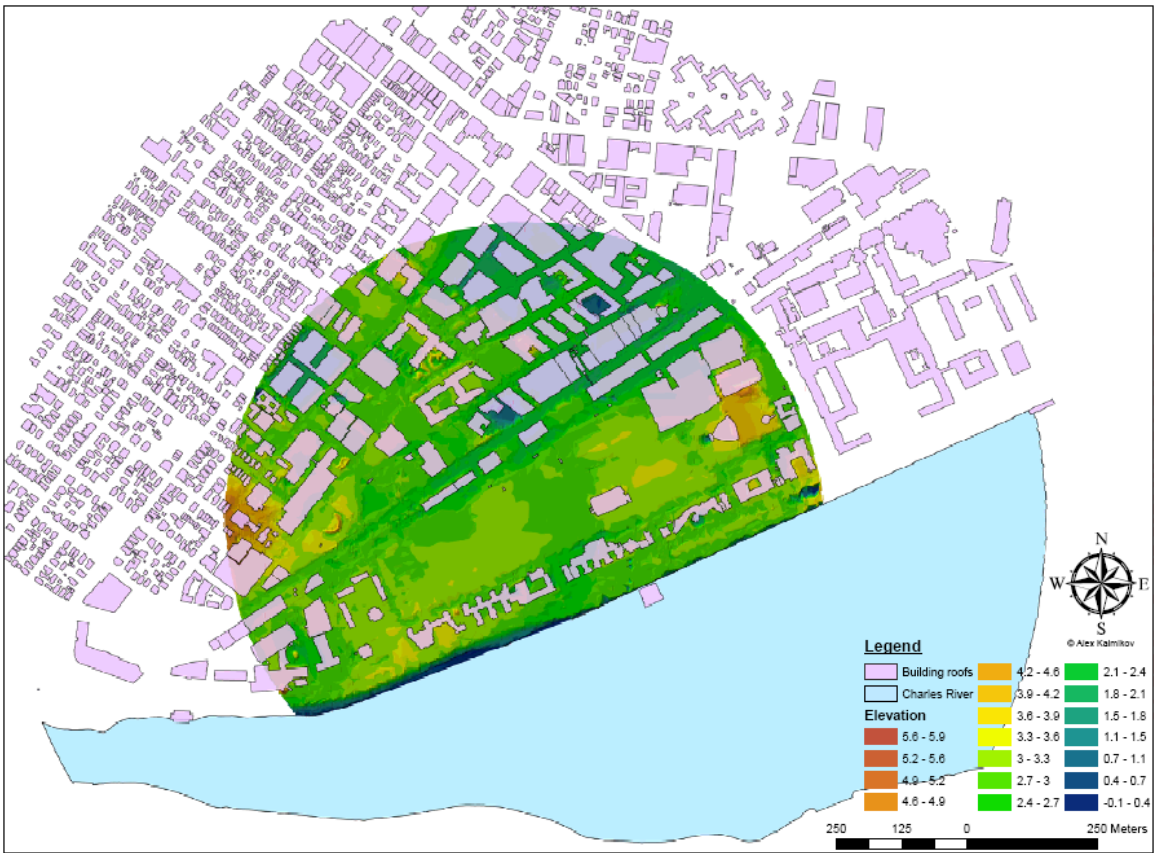

Figure 21: GIS map of MIT campus and the surroundings. Building roofs, river outlines and topography shown.

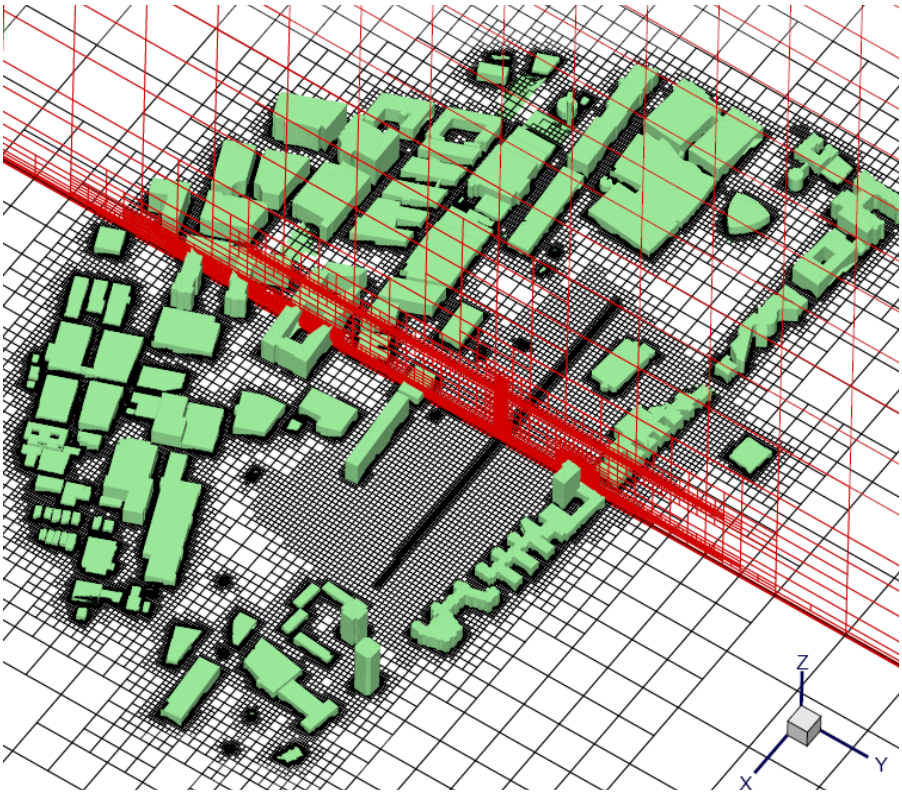

Figure 22: Three dimensional model of campus geometry and CFD grid for inner domain.

Physical Site Analysis

Spatial Analysis

Physical site analysis begins with integration of directional wind statistics with urban GIS data (Figure 23). The directional statistics of the wind are presented as *wind roses*: the radial dimension represents the frequency of wind occurrence in each of the directional sectors. Each sector is divided to represent absolute frequency of observed wind speeds in this direction with speed intervals being represented by a color map consistent between all the figures in this paper. We note that this statistical analysis is based on higher angular resolution (10^o), than what is used for directional CFD calculations in this paper (30^o). Higher angular resolution analysis, therefore, would be expected to provide better match to the measured data by resolving the fine directional structure of wind flow.

It is seen in various figures that the prevailing wind direction at both sites during the 3 months measurement period is West-North-West. This prevailing direction is consistent with Green Building measured statistics for this period but is different from what was found in a previous study[8]. Examination of multi-annual climatology at the Green Building and at Logan Airport confirms the prevalence of Western and North-Western winds, but also allows an explanation for the earlier observation of South-Western winds if the earlier study considered only limited measurement period during late spring.

Detailed qualitative analysis of the integrated GIS map reveals micro-meteorological differences between the two sites. The western site (MT2) exhibits jet and wind tunneling effects, presumably due to acceleration over the open space upwind and channeling by the surrounding buildings through the narrowing entry to the large open area (MIT Brigg's field). High winds of over 8 m/s are observed for 4.4% of the time with a maximum measured wind speed of 13.5 m/s. At the eastern site (MT1), opposite wind characteristics can be observed. Although the average direction of the wind is the same, the angular spread is higher with sensible reduction of occurrence in the central sector. The speeds are lower, rarely reaching 8 m/s (1.1% of the time), with maximum measured wind speed of 12.6 m/s. These observations suggest that the eastern site is subject to turbulence and wind blocking conditions by the upwind buildings and to stagnation pressure at the upwind side of the leeside building – the MIT Tennis Facility.

---

[8] Bates R., S. Fox, K. McCusker, K. Pesce and D. Wesolowski, 2007, *Wind Study: Feasibility Study and Recommendations for Implementing Wind Power on MIT's Campus.* MIT course 5.92 final report.

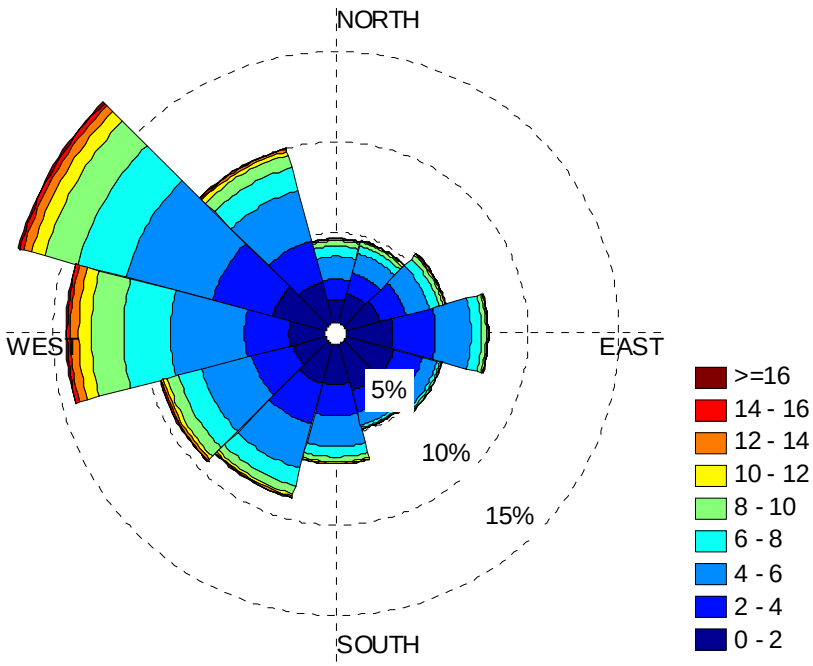

(a): MIT's Green Building.

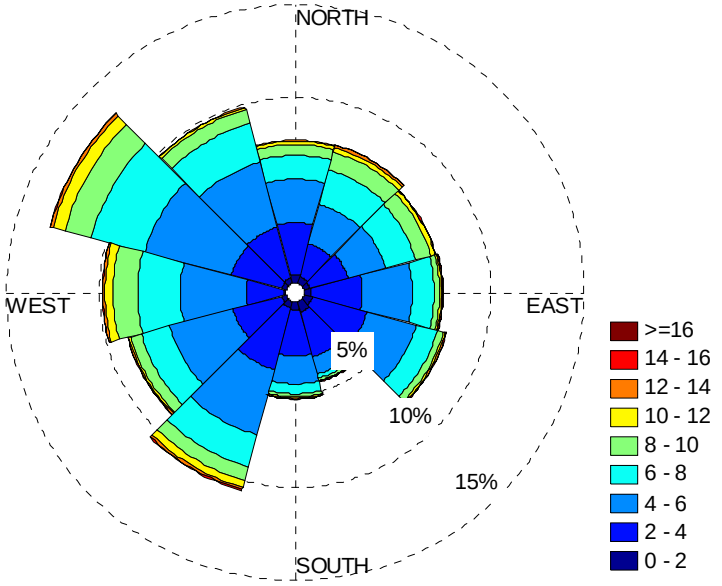

(b): Logan Airport (BOS).

Figure 23: 2 year (2008-9) directional statistics on the roof of MIT's Green Building (a) and Logan Airport (b). Colors represent wind speed, radial extent represents frequency of occurrence (5%, 10%, 15% grid contours shown).

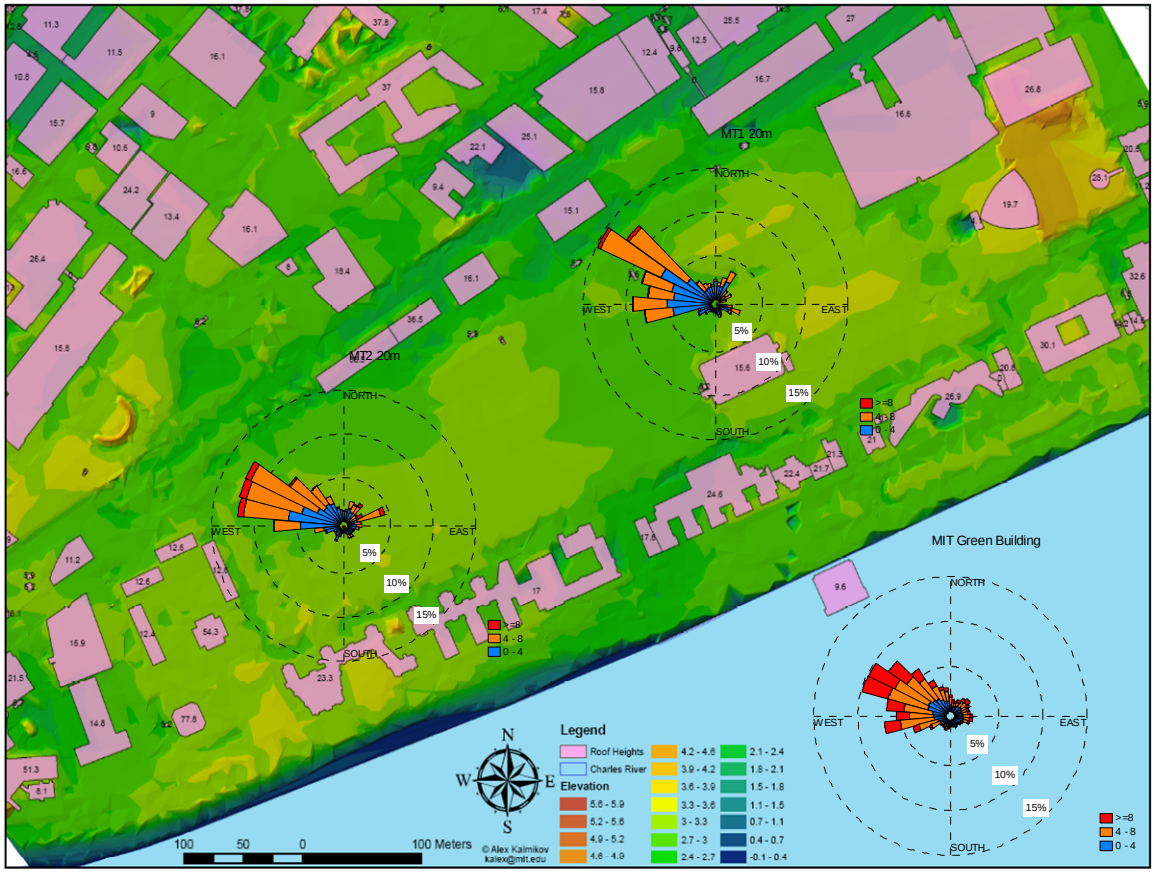

Figure 24: Spatial analysis of wind resource - GIS site map with directional wind statistics at met towers locations

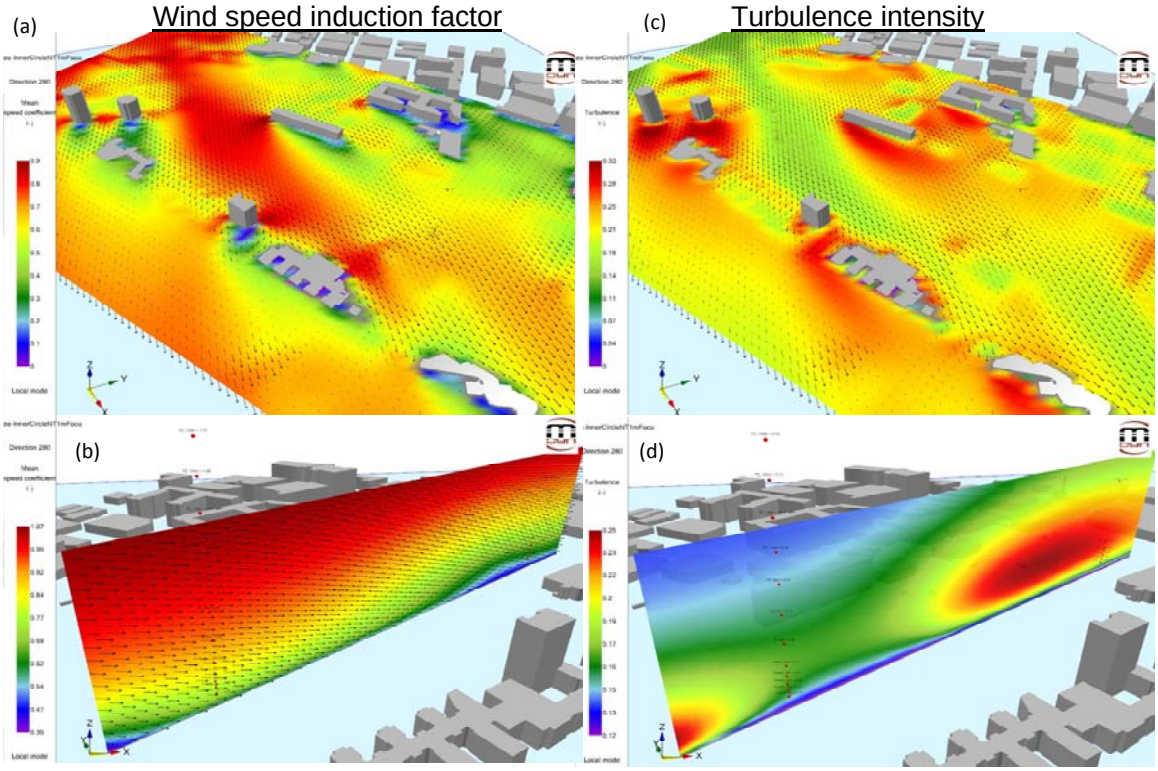

Figure 25: Directional calculation of urban wind induction factors, shown for the prevailing wind direction - 280°

CFD Analysis

CFD simulations confirm these assessments quantitatively for the prevailing synoptic wind direction of 280^0. It can be seen that a high winds channel is formed through the sports field. This area is characterized by lower turbulence (Figure 24 (c), green) and higher mean speeds (Figure 24 (a), red). The CFD simulations reveal the 3 dimensional structure of this flow feature. The high wind channel modifies the vertical shear and brings higher winds closer to the ground, Figure 24 (b). The turbulent area is elevated and localized behind tall buildings' roofs, Figure 24 (d). The western site (MT2) is confirmed to be centered in the high winds channel, the eastern site (MT1) is in the turbulent building wake.

CFD Power Resource Assessment

Local climatology assimilation

We reconstruct the three dimensional structure of wind resource by combining the deterministic CFD calculations with assimilation of real measured wind data statistics. The reconstructed three dimensional wind fields assimilate long term climatology measured at a single location inside the computational domain and extrapolate the statistics of wind resource from this single point to the full extent of the domain. Thus, we obtain the full spatial structure of wind climatology, a four dimensional spatial-stochastic field parameterized in the stochastic dimension by Weibull distribution. The analysis provides three dimensional fields of mean wind speed, Weibull shape (k) and scale (A) parameters, wind power density and turbulence intensity.

To validate this approach we first assimilate climatological data in one of the local measurement points - MT2 20m, and compare the extrapolated estimates for point MT1 20m (located 364m away) with data measured directly at that point. We show the results of assimilation of 3 months of winter measurements data. The input data is shown in Figure 25 (a). On the left side we see a histogram distribution of the measured wind speeds. The mean speed is 4.15 m/s and the corresponding Weibull shape parameter k is 1.963, corresponding to nearly Rayleigh distribution. On the right we see the directional histogram, also known as the wind rose, which shows a clear prevalence of West-North-Westerly winds. Frequency of occurrence of strong winds over 8 m/s is 4.4%. Figure 25 (b) shows the measured statistics at the control point MT1 20m. The directional distribution appears very similar (the coarse angular resolution is hiding the fine details that were discussed in the Spatial Analysis section), but the frequency of high winds is reduced from 4.4% to 1.1%. The mean wind speed is reduced to 3.77 m/s and the Weibull shape parameter k is increased to 2.049. The resulting wind power densities are 82.80 and 58.37 W/m^2 in the assimilation and the control point, respectively. Next, we compare the measured statistics at the control point to the extrapolated estimate, shown in Figure 25 (c). We see that the directional spread is mainly preserved, the extrapolation captures the reduction in occurrence of high winds to 2.6%, the mean speed decrease to 3.74 m/s and wind power density to 61.45 W/m^2. Since the goal of this study is comparison of the wind resource between the two sites, it is convenient to express their difference as the ratios of mean speeds and power densities. The measured ratios are 1.10 and 1.42, respectively. The simulated ratios between the assimilation point and the control point are 1.11 and 1.35. For convenience, these numbers are summarized in Table 4. We conclude that the

result of the assimilation procedure is consistent with the measured trends, which provides a preliminary validation of our approach. We note, however, that the results are not perfect and further work is required to estimate the accuracy of the method and validate the approach against the expected precision.

The method of local Climatology Assimilation (CA) allows extension of the resource assessment procedure from single measurement points to the three dimensional space. The figures shows the horizontal map of wind power density at 20 m above ground, the corresponding vertical cross section of power density is shown. It is seen that site MT2 is located in the region of higher power density. The cross section shows the vertical stratification of the power density and reveals that at the Western site (MT2) the high wind resource is closer to the ground. The mean directionally averaged turbulence intensity is shown. It is seen that the Eastern site (MT1) is located in region that is more turbulent on average. The key characteristic of wind resource is the skewness of its probability distribution. We display it by the corresponding Weibull shape parameter k in the horizontal map and vertical cross section in Figure 27. It is seen that the spatial distribution of this parameter has a complex structure, but at the Western site (MT2) it has clearly lower values, which also explains the higher wind power density at this site.

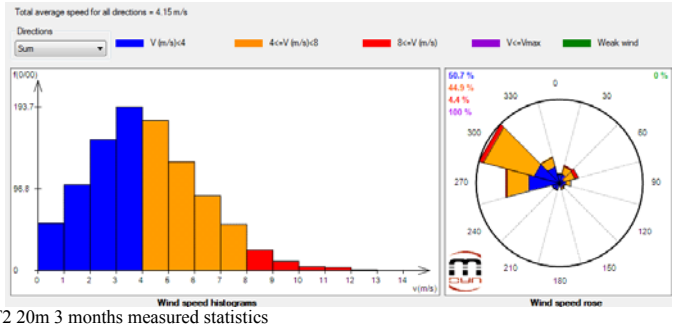

MT2 20m 3 months measured statistics

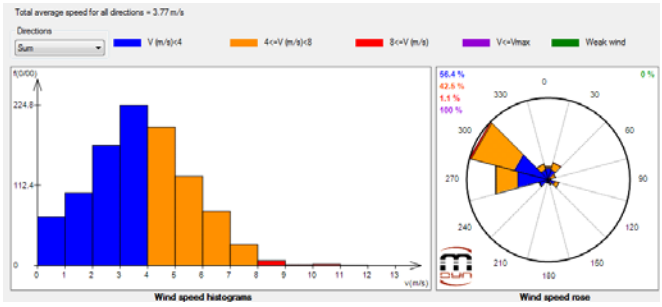

MT1 20m 3 months measured statistics

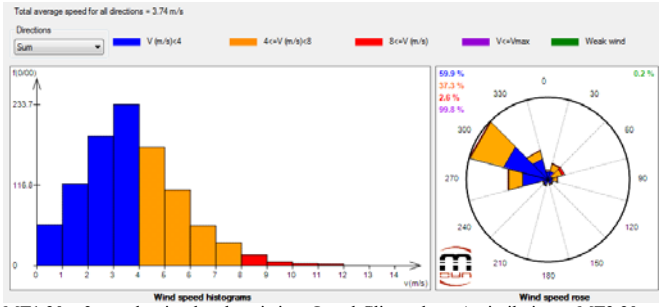

MT1 20m 3 months simulated statistics - Local Climatology Assimilation at MT2 20m

Figure 26: MT 1 local climatology

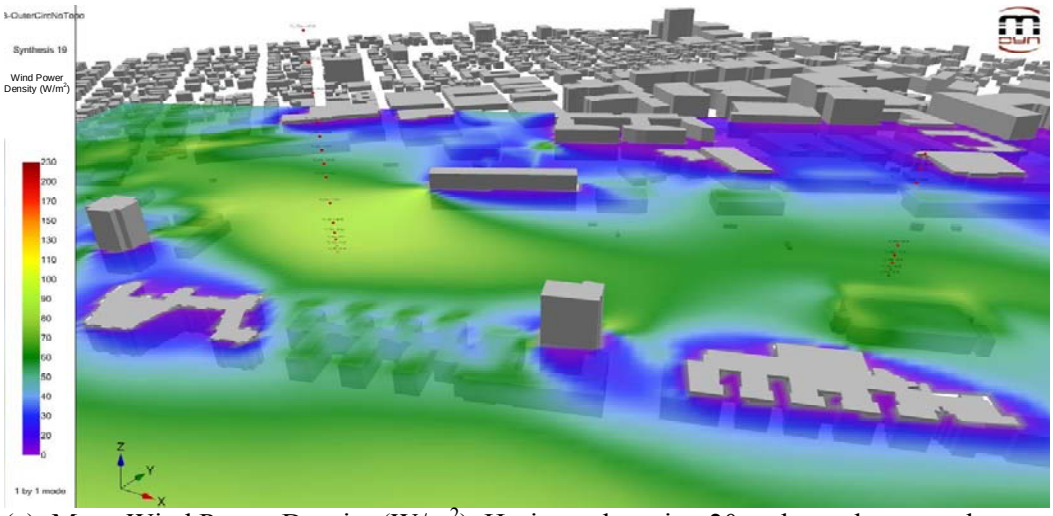

(a) Mean Wind Power Density (W/m^2), Horizontal section 20m above the ground.

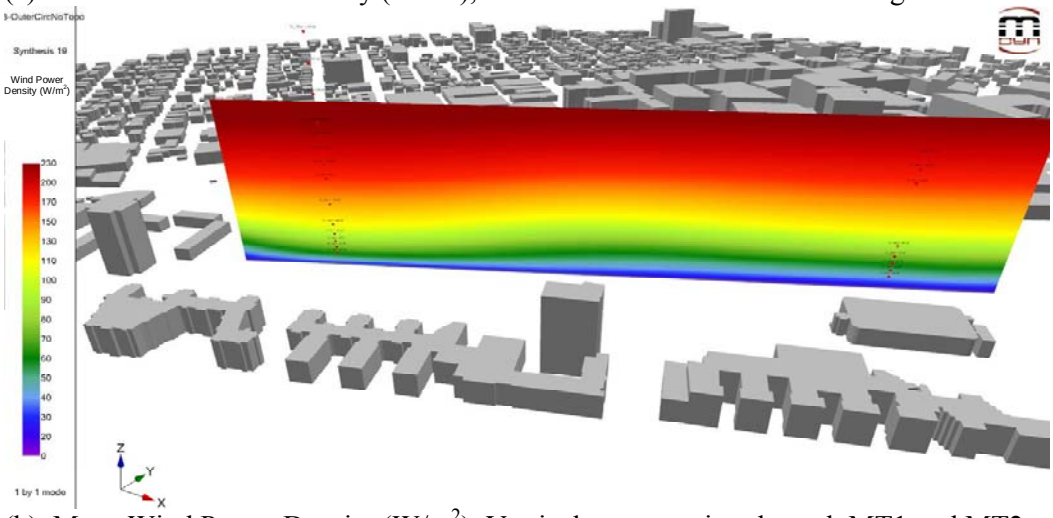

(b) Mean Wind Power Density (W/m^2), Vertical cross-section through MT1 and MT2.

Figure 27: CFD analysis results

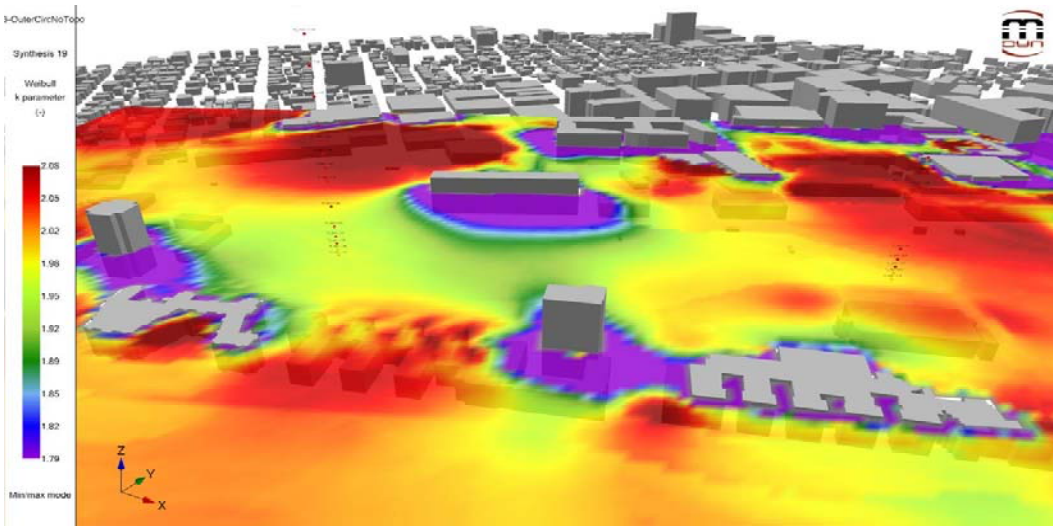

(a) Expected Weibull Shape Parameter k, Horizontal section 20m above the ground.

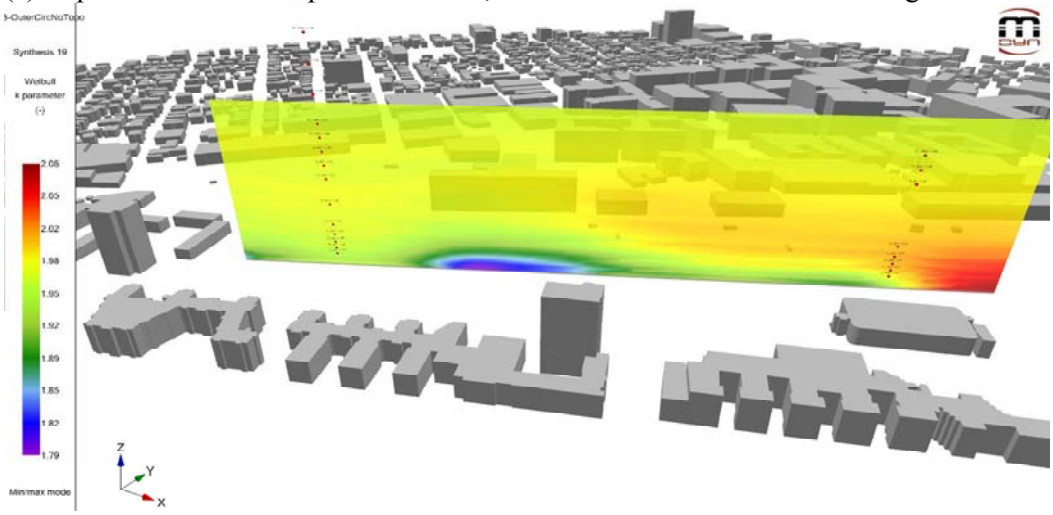

(b) Expected Weibull Shape Parameter k, Vertical cross-section through MT1 and MT2.

Figure 28: CFD results

Background climatology assimilation

The local Climatology Assimilation was performed to reconstruct the best estimate of spatial wind resource statistics and was possible due to existence of locally measured wind climatology. In practical applications, when locally measured wind climatology is not available, the Climatology Assimilation procedure allows reconstruction of spatial wind resource statistics by assimilation of background climatology. We assume that the measurements at the roof MIT's Green Building represent the background climatology for MIT campus area and assimilate it 90 m above the Eastern site MT1. The assimilation was performed for 3 months of local measurement period and for 2 years of data starting from April 2008. The climatological parameters are shown in Table 3. The histogram and the angular distribution of wind speeds for these two periods are shown above.

Table 3: Assimilated wind power parameters based on the Green Building roof data.

	3 months	2 years
Power Density (W/m^2)	221.78	126.54
Mean Speed (m/s)	5.16	3.96
Weibull Shape k	1.409	1.284

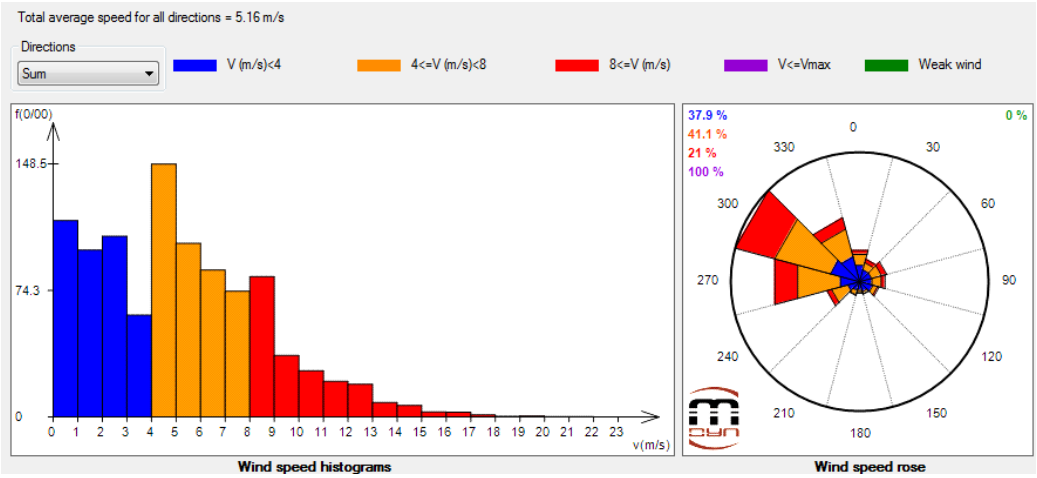

(a) 3 months statistics

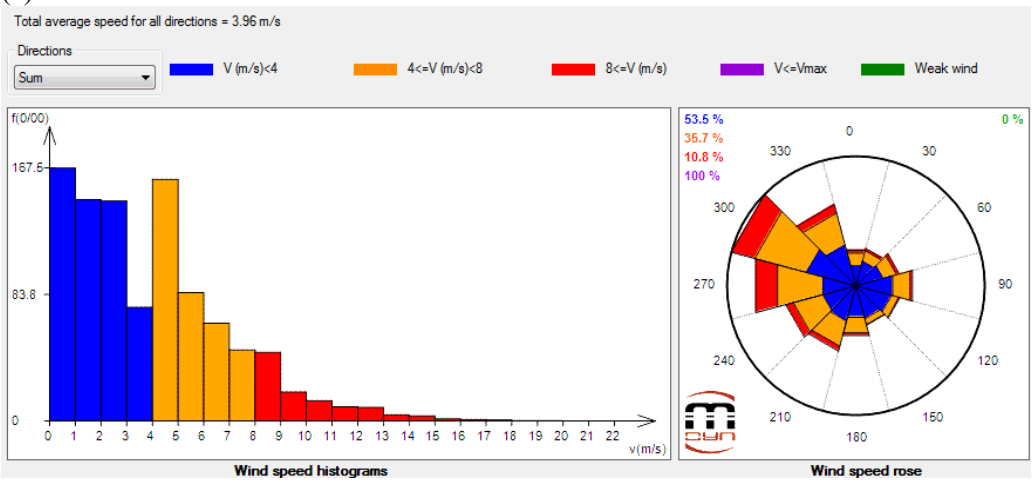

(b) 2 years statistics

Figure 29: Input climatology for background Climatology Assimilation at MT1 90m

Table 4: Comparison of the measured and the simulated wind power parameters. The first column is the measured data at MT2 20m point and is the input to the Local CA reconstruction procedure at this point. It is compared to the second and the third columns – the measured and the reconstructed data at the control point (MT1 20m), respectively. The next columns present the reconstructed results at the two points for assimilation of the background measured data during 3 winter months (Background CA 3 months), MCP normalization to 13 years airport data and assimilation of 2 years of background data. For convenience of comparison, the ratios of power density and mean speeds between the two points are shown for each reconstructed and measured pair. For further discussion see the text in the next section.

	Measured 3 months		**Local CA 3 months**	**Background CA 3 months**		**MCP normalization 13 years**		**Background CA 2 years**	
	MT2 20m	MT1 20m	MT1 20m	MT1 20m	MT2 20m	MT1 20m	MT2 20m	MT1 20m	MT2 20m
Power Density (W/m^2)	82.80	58.37	61.45	71.15	99.03	39.43	46.49	41.92	51.74
Mean Speed (m/s)	4.15	3.77	3.74	3.54	3.87	3.26	3.38	2.73	2.86
Weibull Shape k	1.963	2.049	2.008	1.446	1.378	2.041	1.935	1.281	1.231
Power Ratio	1.42		1.35	1.39		1.18		1.23	
Speed Ratio	1.10		1.11	1.10		1.04		1.05	

Comparison of Resource Assessment techniques

The results of the different resource assessment techniques are summarized in Table 4. All the methods agree that the wind resource at MT2 is better, the differences can be conveniently quantified by the ratios of the available wind power densities and mean wind speeds. It is seen that the local CA approach gives the best estimates when compared to the measured data. The 3 month background CA recovers the proper ratios although the absolute values of wind power density are higher. The 2 year background CA and 13 year MCP normalization produce comparable ratios and power densities, although the mean wind speed are significantly different. We explain this discrepancy by the different Weibull shape parameters k in these two calculations. The significantly lower values of k in the background CA are the responsible for the skewness of power density distributions and higher values of their integrals.

Conclusions

Referring back to Tables 1a and 1b in the introduction which summarize the performance of the two sites, neither site is particularly well suited to wind development of a Skystream 3.7 turbine. The capacity factors for different heights and sites range from 4 to 10% and the operational time is expected to be less than 50% in most cases. This means that 50% of the time, the turbine will not be operating and this will be seen by those living near the turbine or visiting campus. The turbine will also be subjected to a fair amount of turbulent wind which may affect load and fatigue for the turbine in the long term. The estimated turbulence intensity for the two sites are quite high (double that of clear flat land). Turbulent wind means that the speed and direction of the wind is constantly changing, often faster than the system is designed to react. Thus, the turbine will have to endure loading that is perhaps asymmetric or complex which could affect the long-term maintenance of the turbine. However, as a research tool, having a turbine placed in either location would be interesting. A turbine in such complex terrain provides a good basis for research at the forefront of our current understanding for small urban wind. The use of CFD analysis as shown above is just one of the many avenues that holds potential for turning a campus turbine into a living research project. If the decision is to go ahead with a turbine, the second of the two sites is expected to perform slightly better than the first in terms of energy production, but this could prove marginal when compared to other site selection criteria such as the cost of installation and maintenance and the visual and acoustic impacts.

B. *Wind Turbine Interconnection and Monitoring*

Updated as of March 1, 2010

Kevin Ferrigno, MS Candidate, Engineering Systems
Bryan Palmintier, PhD Candidate, Engineering Systems

Connection of Wind Turbine to MIT Campus Utility Network

The first task of the integration process was to identify the potential connection points to electrical sufficient electrical loads. The MIT campus is served by the MIT Facilities Department which distributes electricity to campus buildings through 13.8 kV distribution network. Each building or complex receives the 13.8 kV utility service and steps down the voltage to the standard 208/120 VAC. The Skystream wind turbine's output is 2 phases of standard 3 phase 208 VAC arrangement. This voltage is compatible with each building after the step down transformation of the incoming power feed at each building. Thus, the connection points considered were the utility rooms of nearby buildings. [1]

Potential connection points were evaluated based on distance from the turbine and the landscape between the turbine and the connection point. For example, Simmons hall is fairly close to the Westgate location, but lies across Vassar Street from the turbine. Thus, installation of the power connection to Simmons Hall would require building a trench under Vassar Street or running in existing conduit which also carries 13.8 kV AC power. Digging a trench under a city owned street requires extensive coordination with the city and add significant cost as the street must be repaired after construction. Also, running the 208 VAC power in the same conduit as 13.8 kV AC power requires the 208 VAC power feed to use the same cable that is required for 13.8 kV AC power. This was also determined to be cost prohibitive. [1]

For the location in Steinbrenner stadium, the best interconnection point was determined to be the electrical building that services the campus Tennis Bubble. This connection could be made through a 250 foot trench and conduit that runs almost entirely under grass. For the location near the Westgate parking lot, the best interconnection point was determined to be the nearest low rise building of the Westgate complex. The trench and conduit for this location would pass under the Westgate parking lot and Amherst Street. Since Amherst Street is owned by MIT, this does not add as much expense to the project as a connection to Simmons Hall would. [1]

Load profiles for individual buildings were not required. In the unlikely event the building's power load fell below the 2.4 kW output of the turbine, the excess power will feed back through the transformers into the MIT utility loop without damaging equipment or the Wind Turbine. Because the turbine connects to the MIT utility loop, obtaining permits with the local utility company are not required for grid connection.

For each location, the run of the connection will be about 250 feet from the tower to the utility connection points. Adding in the 60 foot height of the tower, the total run will be

310 feet. For runs over 264 ft, including tower height, the Skystream Owner's Manual recommends running 6 AWG wire from a base mounted electrical disconnect box to the utility panel where the Skystream wind turbine will connect to the campus grid. There will be a second disconnect point in the utility room so that the wind turbine can be disconnected from the grid to either facilitate work in the utility room. [2]

A trench will be dug from the turbine to the interconnection point. The trench will contain two PVC pipes. One will serve as conduit for the electrical power connection. The second will contain wiring for the data collection system. Once placed, the trench will be back filled, the conduits capped with a concrete barrier (to prevent accidental puncture from normal use of the surfaces above the trench) and then the surface (grass or pavement) will be replaced. [1]

Data Collection

The Skystream provides power output data through a wireless Zigbee communication. [3] To support research use of the turbine and data, a permanent wind speed data collection system at the turbine is being considered. One guideline for required instrumentation is the Massachusetts Technology Collaborative's guidelines for wind measurement used to obtain the incentives available for micro wind turbine installations. The summary of the measurement requirements is shown in the following table.[4]

Table 5: Instrumentation recommendations

Measurement-Instrument	Recommended Location	Comments
Wind Speed - Anemometer	Primary at 1 Rotor Diameter below Hub Height. (About 48 feet above ground) Secondary at 1.5 – 2 Rotor diameters below hub height. (About 36-42 feet above ground)	May want to mimic assessment configuration of 2 anemometers and wind vane at each height.
Wind Direction – Wind Vane	0.5 – 1 Rotor Diameter Below Primary Anemometer	
Temperature	On Wind Vane Boom	
Turbine Power - Watt Transducer	In Utility Room	
Data Logger	In Weatherproof Enclosure at Tower Base, Utility Room, or Data Room	

Another alternative would be to duplicate the instrumentation used during the wind assessment performed for this project. This configuration uses two anemometers and a wind vane at each of 2 different measurement heights on the tower.

This data will be available in real time display via a web interface or to a kiosk location in a public area such as the student center. This will require the data logger to allow real time access by a PC or direct capability to write to an online database. This will allow real time data capture and report the data on a continuous basis to an active database.

Further development for the data collection system including costs and equipment will be determined in the next phase of the project.

Operation and Maintenance

According to the Skystream Owner's Manual, the turbine requires no regular maintenance in the first 20 years of operation. Yearly visual inspections of the turbine are suggested as a way to verify the integrity of the wind turbine blades. [2] In winter, there is a danger of ice formation on the turbine blades, thus, during weather where ice buildup is possible, the turbine should be monitored. If ice buildup occurs, the turbine should be disconnected from the MIT utility grid, shutting down the turbine. [2] For unscheduled maintenance requiring access at the top of the tower, a bucket truck will be required to work on the wind turbine on top of the 60 foot tower. Both potential locations for the wind turbine should provide suitable access for this work if it is ever required. [1]

References

[1] Cooper, Peter. Personal Communication.
[2] Renewable Energy Trust. *Wind Incentive Program. Attachment E: Wind Project Monitoring Requirements.* http://www.masstech.org/wind/micro_wind/AttachmentE_MonitoringReqs.pdf. Accessed 1 March 2010.
[3] Southwest Windpower. 2009. *Skystream 3.7 Owner's Manual 60 HZ (North America) Edition*. December 2009. http://www.windenergy.com/documents/manuals/3-CMLT-1054_Skystream_Manual.pdf. Accessed 1 March 2010.
[4] Southwest Windpower. 2007. *Skystream 3.7 Interface & Software Guide*. October 2007. http://www.windenergy.com/documents/manuals/3-CMLT-1061_Skystream_Interface_&_Software_Guide.pdf. Accessed 1 March 2010

C. *Pre-Construction Environmental Impact Considerations*

Updated as of May 18, 2010

Mark Lipson, PhD Candidate, Civil Engineering

Overview

For reasons of efficiency and land availability, utility-scale wind farms tend to be located along elevated ridges, in open plains, or off coastlines. However, smaller installations in urban areas are also becoming more popular as a supplementary source of wind power capacity as demand increases [29]. A benefit of urban wind power is that by building on already-developed land, risks to wildlife and the environment should be reduced. Less natural habitat is destroyed, and sensitive wildlife are likely already to have been displaced.

At large wind installations, pre- and post-construction environmental reviews are important components of the planning and evaluation processes, and many such studies have now been completed. As a rough average, a single large turbine might account for 0-3 bird fatalities and 5-15 bat fatalities per year, although these numbers are variable from site to site [10, 20]. Still, even in the most serious examples documented thus far, bird fatalities in particular have been minor as compared to those caused by buildings, power lines, vehicles, and pets [21, 30]. Given the limited scope to date of urban wind, very little specific work has been done on environmental impacts in developed areas, but extrapolating previous results to cities, it would appear that risks to wildlife should be fairly small.

We have contacted the Massachusetts Natural Heritage and Endangered Species Program (NHESP), and an official with NHESP has advised us that our project does not require any formal environmental review. Moreover, given the scale and location, no special measures are necessary for mitigation of risks to wildlife (A. Coman, personal communication). In addition, representatives of Mass Audubon have advised us that site-specific monitoring would not be necessary, as a small turbine in an urban setting should cause little harm (J. Clarke and B. Poor, personal communication). In accordance with their recommendations, we present below, in lieu of a long-term field study, an analysis of potential risks based on previous knowledge of the Cambridge area and a thorough review of the wind-wildlife literature.

Resident birds

Most of the resident birds in cities like Cambridge are of little conservation concern, being widespread as a result of their tolerance of human disturbance. However, there are some exceptions, most notably raptors (hawks and falcons), which are often willing to live and nest among human-made structures and take advantage of the abundant small-animal prey [7]. Urban raptors are generally native species, have low population densities, and in some cases are threatened or declining in their natural ranges. Also, despite the benefits of cities, raptors there are at risk of collision with vehicles, windows, and power lines [7].

Raptors, especially local residents, have been found killed at a number of wind farms in the US and Europe, although there is also evidence that they learn to avoid turbines [18, 27]. By far the worst and most prominent raptor fatalities at a US wind facility have been those that occurred at Altamont Pass in California around 20 years ago, where surveys found several hundred raptors killed per year, including red-tailed hawks and American kestrels, both of which nest in Cambridge [30]. Red-tailed hawks there were most at risk when hunting or kiting in strong winds over certain hill slopes, and otherwise they tended to avoid the turbines [12, 30]. Overall, it appears that a number of specific features of Altamont made it particularly dangerous, and the experience there should not serve as a guide for a single, small turbine in a very different location [6, 10, 12, 27]. As an example, red-tailed hawks and bald eagles have nested without incident within a quarter mile of the Erie Shores Wind Farm in Ontario, and many other raptors have been observed passing safely nearby, with only one fatality recorded in two years [15]. At newer installations in particular, risks to species such as kestrels appear to be minimal [10].

In Boston and Cambridge, the most sensitive resident birds are peregrine falcons, which are state-listed as endangered in Massachusetts [23]. Two pairs of peregrines currently nest within a little over a mile of the MIT athletic fields (G. Dysart, personal communication). Peregrine falcons are known to have been killed in collisions with wires [19, 27], but only a few wind-related fatalities have ever been documented, all in Europe [11, 19, 30]. A pair has even nested safely on one occasion only 250 meters from active turbines [30]. NHESP is not aware of any precautions having been necessary for past construction on account of peregrines in the Boston area and would not require any in our case (A. Coman, personal communication).

Migratory birds

Several groups of birds migrate through eastern Massachusetts in the spring and fall. The most prominent are the more than 100 species of songbirds that breed in the fields and forests of New England and Canada and winter in the tropics. These songbirds migrate almost exclusively at night, generally at least 400-500 feet above ground [1, 5, 18]. Several parks in Boston and Cambridge are heavily used as daytime stopover areas, including Fresh Pond and Mount Auburn Cemetery, both of which are designated as Important Bird Areas [24]. However, these two sites are more than two miles from the proposed turbine locations, and there is no high-quality habitat within a mile. Waterfowl and raptors also migrate through the region, but like songbirds, they fly well above most buildings and do not congregate at any locations close to MIT [18].

Despite their generally high flight altitudes, nocturnally migrating songbirds can face risks from human-made structures. Many birds are killed at communications towers and at skyscrapers, particularly in the presence of bright lighting and on nights with fog or otherwise poor visibility [21]. However, most wind turbines, and certainly small-scale installations, are too low to be a danger, and there have been no reports of any significant songbird mortality at wind farms, even on nights when some birds have been observed flying at turbine heights [10, 14, 30].

Bats

In addition to birds, bats have been found killed at many wind farms worldwide, although researchers are still not sure how and why bats are killed by turbines [13]. Particularly high mortality rates have been observed at several installations in the Appalachians [20, 28]. There and in other parts of eastern and central North America, the large majority of fatalities have come in the fall and have been from three migratory species, eastern red bats, hoary bats, and silver-haired bats [4, 14, 20]. In Europe, mortality rates have been lower, especially at shorter turbines, with only a few instances of deaths at residential-scale installations [17, 26].

Relatively little is known about the distribution, behavior, and especially the migration patterns of bats. Bats are believed to migrate mostly above 300 feet, and most collisions have been reported at large turbines, especially those 200 feet and taller [5]. Some have hypothesized that fatalities tend to represent actively migrating individuals, rather than those foraging closer to the ground [10], while others believe that bats are at risk due to their attraction to tall landmarks as a means of navigation and flock coordination [9].

The three highest-risk species of bats listed above breed in woodlands, prefer less-disturbed habitats, and are uncommon in the Boston area [3, 22]. However, in the fall, some individuals of all three species migrate southward along the Massachusetts coast [8, 25], with some likely passing through Boston (T. Kunz, personal communication). Still, almost all bats found in Massachusetts cities are little brown bats and big brown bats [22], both of which are common and of relatively little conservation concern. Moreover, the foraging behavior of little brown and big brown bats leads to their rarely being killed by turbines [4], even at locations where they are known to be active nearby [10].

Case studies

As discussed above, research on small-scale wind projects and those in urban areas is limited. No detailed environmental studies have been conducted at small turbines in eastern Massachusetts, but several individuals have been willing to share informal observations. Among a Northwind 100 turbine in Medford, three turbines of varying size in Hull, and the multi-turbine installation at the Museum of Science in Boston, no bird or bat fatalities have been reported (P. Barry, A. Stern, and D. Rabkin, personal communications).

At least two relevant studies have been completed in the eastern Great Lakes region. In 2007, a 10 kW, 36 m turbine was installed at the Tom Ridge Environmental Center in Erie, Pennsylvania, one of several similar turbines at educational centers statewide [2]. The site in Erie was suburban in character. In the course of a year of monitoring, no dead bats were found, and the only bird fatality was a common grackle that appeared to have died from natural causes. Additionally, no mortalities were reported from the other centers. A fair number of birds were observed in the surrounding area and migrating

overhead, but it seemed as though they either actively avoided the turbine or otherwise stayed out of danger [2].

In Toronto, a 750 kW, 94 m turbine was installed at the Canadian National Exhibition grounds, a more urban setting, in 2002 [16]. Carcass searches were conducted during the spring and fall migration seasons in 2003. Despite the presence of Lake Ontario nearby, only two dead birds were found, a European starling and an American robin. Migrant songbirds were observed around the grounds, along with resident birds such as gulls and Canada geese, and a single American kestrel was spotted twice in flight. Again, though, the birds seemed to avoid the danger [16].

Acknowledgments

I would like to thank Jack Clarke and Banks Poor from Mass Audubon for their guidance and Amy Coman, Thomas Kunz, Patricia Barry, David Rabkin, Andrew Stern, and Greg Dysart for providing much helpful information.

References

[1] Allison, T. and Clarke, J. A challenge proposal regarding the Cape Wind energy project. Mass Audubon, 2006.
[2] Andersen, K. A Study of the potential effects of a small wind turbine on bird and bat mortality at Tom Ridge Environmental Center, Erie, Pennsylvania. Prepared for the Pennsylvania Department of Conservation of Natural Resources, 2008.
[3] Animal Diversity Web (http://animaldiversity.ummz.umich.edu/site/index.html). University of Michigan Museum of Zoology, 2010.
[4] Baerwald, E. Prairie winds: migrating bats and wind energy in Canada. BATS Magazine **25:3** (2007), 1-4.
[5] Barclay, R., Baerwald, E., and Gruver, J. Variation in bat and bird fatalities at wind energy facilities: assessing the effects of rotor size and tower height. Canadian Journal of Zoology **85** (2007), 381-387.
[6] Cape Wind draft EIS executive summary. US Army Corps of Engineers, 2004.
[7] Chace, J. and Walsh, J. Urban effects on native avifauna: a review. Landscape and Urban Planning (2004).
[8] Cryan, P. Seasonal distribution of migratory tree bats (Lasiurus and Lasionycteris) in North America. Journal of Mammology **84:2** (2003), 579–593.
[9] Cryan, P. and Brown, A. Migration of bats past a remote island offers clues toward the problem of bat fatalities at wind turbines. Biological Conservation **139:1-2** (2007), 1-11.
[10] Erickson, W. et al. Synthesis and comparison of baseline avian and bat use, raptor nesting and mortality information from proposed and existing wind developments. Prepared for the Bonneville Power Administration, 2002.
[11] Everaert, J. Wind turbines and birds in Flanders: preliminary study results and recommendations. Natuur. Oriolus **69:4** (2003), 145-155.
[12] Hoover, S. The Response of red-tailed hawks and golden eagles to topographical features, weather, and abundance of a dominant prey species at the Altamont Pass Wind Resource Area, California. NREL, 2002.

[13] Horn, J., Arnett, E., and Kunz, T. Behavioral responses of bats to operating wind turbines. Journal of Wildlife Management **72:1** (2006), 123-132.
[14] Howe, R., Evans, W., and Wolf, A. Effects of wind turbines on birds and bats in northeastern Wisconsin. Prepared for the Wisconsin Public Service Corporation and Madison Gas and Electric Company, 2002.
[15] James, R. Erie Shores Wind Farm, Port Burwell, Ontario: fieldwork report for 2006 and 2007 during the first two years of operation. Report to Environment Canada, Ontario Ministry of Natural Resources, Erie Shores Wind Farm LP-McQuarrie North American, and AIM PowerGen Corporation, 2008 (as cited in [18]).
[16] James, R. and Coady, G. Exhibition Place wind turbine report on bird monitoring in 2003. Report to Toronto Hydro Energy Services Inc. and WindShare, 2003.
[17] Jones, G. et al. Determining the potential ecological impact of wind turbines on bat populations in Britain. Prepared for the Bat Conservation Trust, 2009.
[18] Kerlinger, P. and Guarnaccia, J. Phase I avian risk assessment: Mount Wachusett Community College wind energy project. Curry & Kerlinger LLC, 2008.
[19] Kingsley, A. and Whittam, B. Potential impacts of wind turbines on birds at North Cape, Prince Edward Island. Bird Studies Canada, Atlantic Region, 2001.
[20] Kunz, T. et al. Ecological impacts of wind energy development on bats: questions, research needs, and hypotheses. Frontiers in Ecology and the Environment **5:6** (2007), 315–324.
[21] Leahy, C. Kill the lights, save the birds. Mass Audubon Connections **7:1** (2009), 2-3.
[22] Living with wildlife: Bats (http://www.massaudubon.org/Nature_Connection/wildlife/index.php?subject=Mammals&id=20). Mass Audubon, 2010.
[23] Massachusetts list of endangered, threatened and special concern species (http://www.mass.gov/dfwele/dfw/nhesp/species_info/mesa_list/mesa_list.htm). Massachusetts Division of Fisheries and Wildlife, 2008.
[24] Massachusetts Important Bird Areas (http://www.massaudubon.org/Birds_and_Birding/IBAs_new/index.php). Mass Audubon, 2010.
[25] Mass Audubon / Wellfleet Bay Wildlife Sanctuary wind power feasibility study. Mass Audubon with the Energy Consumers Alliance of New England, 2008.
[26] Micro-turbine bat mortality incidents, received by the Bat Conservation Trust. Bat Conservation Trust, 2007.
[27] Ontario Peregrine Falcon Recovery Team. Draft recovery strategy for peregrine falcon (Falco peregrinus) in Ontario. Prepared for the Ontario Ministry of Natural Resources, Peterborough, Ontario, 2009.
[28] POWIWD-V: Proceedings of the onshore wildlife interactions with wind developments: Research Meeting V. Lansdowne, VA November 3-4, 2004. Prepared for the Wildlife Subcommittee of the National Wind Coordinating Committee by RESOLVE, Inc., Washington, DC, Susan Savitt Schwartz, ed, 2005.
[29] Stankovic, S., Campbell, N., and Harries, A. Urban wind energy. London: Earthscan, 2009.
[30] Wind turbine environmental assessment: appendix B, wildlife impacts. Prepared by Dillon Consulting Ltd. for TREC and Toronto Hydro, 2000.

D. Community Considerations: Acoustic and Visual Impacts

Updated as of March 1st 2010

Sungho Lee, PhD Candidate, Mechanical Engineering

Shadow Flicker

During the day time, the rotating wind blades cast rotating shadows on lands, which can be varying over time and location and might affect residential area near by the wind turbine. Depending on the seasons and weather conditions, the significance of shadow flicker can be varying in terms of shadow's rotating frequency and the magnitude of sharpness, which are the main two components that human perception is based on. In other words, the flickering shadow will not be observed if the blade is not rotating or if the weather is cloudy.

Figure 30: Illustration of flicker process

When the sun and the wind blades are collinear such a way that the shadow behind the turbine is shedding onto the building, we can encounter the shadow flickering, which happens at particular times of the day and year. The extent of this impact can be analyzed by geometric characteristic of the potential site and time record of the seasonally varying sun trajectory in a local coordinate.

Analysis Assumptions:

(1) The wind speed is assumed constant as a mean speed (i.e. no seasonal variation of wind speed)

(2) The wind blades are rotating in a constant rotational speed that is corresponding speed to the mean wind speed

(3) The wind turbine blade is considered to be a 2-dimensional circular disk element by its swept area.

(4) The disk element is always normal to the sun light direction

(5) The weather is in a perfect condition with a sufficient sun light all time during the day, and the sky is 100% clear with no allowance for mist, fog, cloud etc.

(6) There are no obstacles along the line of sight between the receiver and turbine blade

(7) The Sun can be considered as a point light source

(8) The sun has to be 5 degrees above the horizon in order to be seen and creates shadow

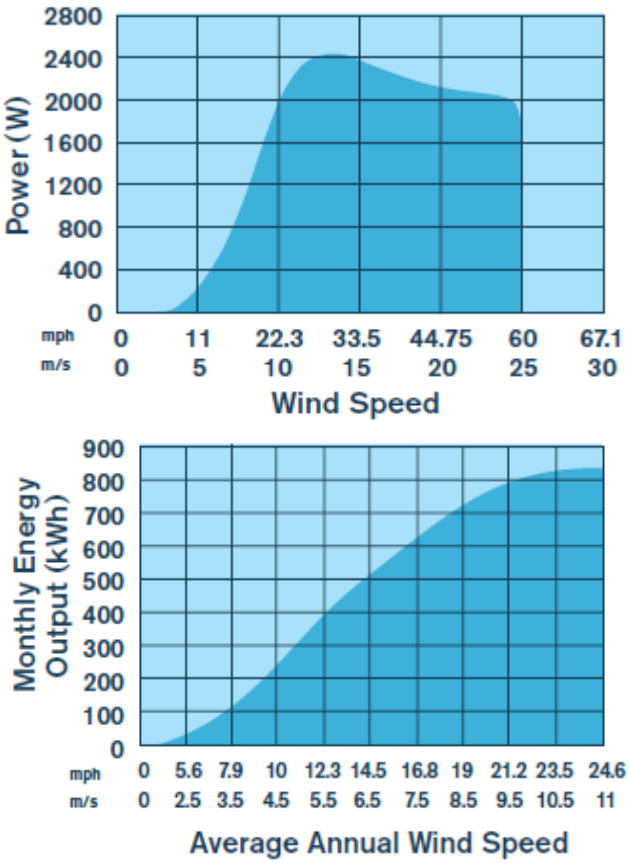

Figure 31: Power curve and monthly energy output for a Skystream 3.7

The dark area at each plot represents where the turbine is actually operating for. As seen above, the turbine starts operating from the wind speed of 3.5 m/sec (cut-in speed) and stops operating for the speed over 63 m/sec (survival speed). The corresponding rotation speed of the blade has been tabulated below.

Table 6: Rotation speed of rotor for different wind speeds from *SkyStream3.7*

	Cut-in	Survival
Wind speed [m/sec]	3.5	63
Rotation speed of rotor [rpm]	50	32.5

The average wind speed over the current site at MIT campus is around 5 m/sec and the corresponding rotational speed of rotor is about 57 rpm, 0.95 Hz. Since the *SkyStream3.7* is a 3-bladed machine, the actual frequency of shadow flicker however is 3 times as high as the rotor speed. Therefore the wind turbine considered for this project has a rotor speed resulting in a shadow flicker frequency 2.85 in average.

Table 7: Level of noise and perception to human population

Flicker Rate (Hz)	Human Perception	RPM of 3 Bladed Turbine (RPM)
<2.5	Negligible	<50
2.5-3	May affect 0.25% of population	50-60
3-10	Effect is perceivable	60-200
10-25	Greatest sensitivity	200-500
>50	Continuous light source	>1000

(Source: *'The Urban Wind Energy', Stankovic, Cambell, Harries*)

There has been a scientific study and analysis about impact of the frequencies of light flicker on human. This result has been obtained from both the general population and the 2% who suffer from epilepsy. As seen in the table above, the wind turbine for this project can possibly affect 0.25% of population with a very minimal impact. The sun path record throughout the year on MIT campus has been obtained and plotted as shown below.

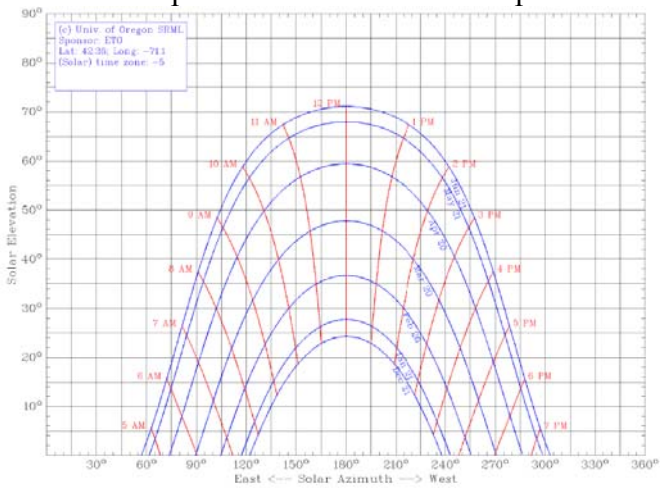

Figure 32: Sun path record for MIT campus from Jan – June

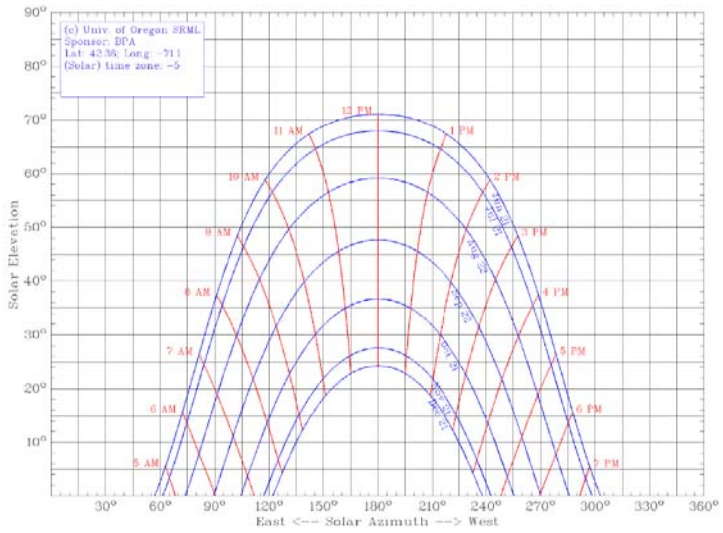

Figure 33: Sun path record for MIT campus from July – December

(**Source**: *Sun path chart program, Solar Radiation Monitoring Lab., Univ. of Oregon*)

The computation of shadow flicker has been determined by modeling the movement of the sun throughout the year. The location of wind turbine and tower height are input to this module, which is set to be at two particular locations over the Briggs field with 20m high each. The information of sun trajectory in terms of elevation and azimuth are adopted and modeled from the record in previous page, and the calculation of location of shadow flicker become possible by drawing a straight line aligned between the sun, turbine and ground receptor. A computational representation of Briggs field, sun trajectory throughout the year and shadow topography on the ground has been plotted below. This enables the representation of shadow topography for any arbitrary sited turbine of 20m high in particular.

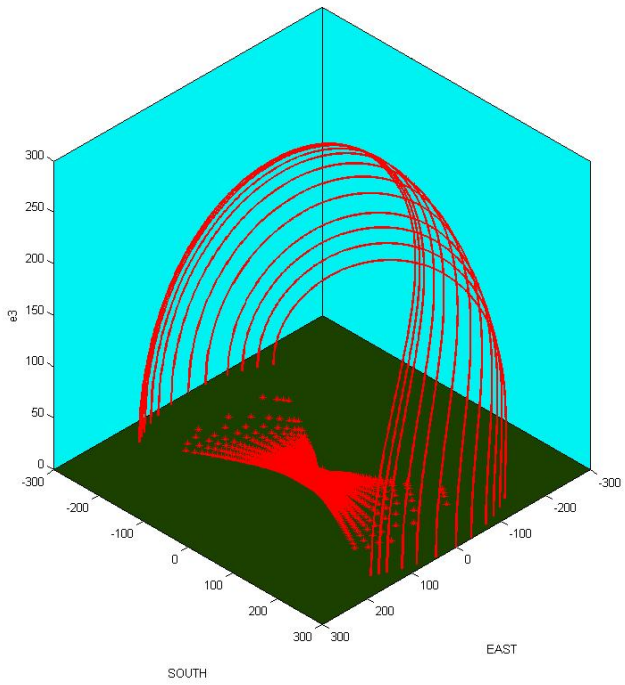

Figure 34: A computational representation of the MIT Briggs field, sun trajectory and shadow topography on the ground [3D VIEW]

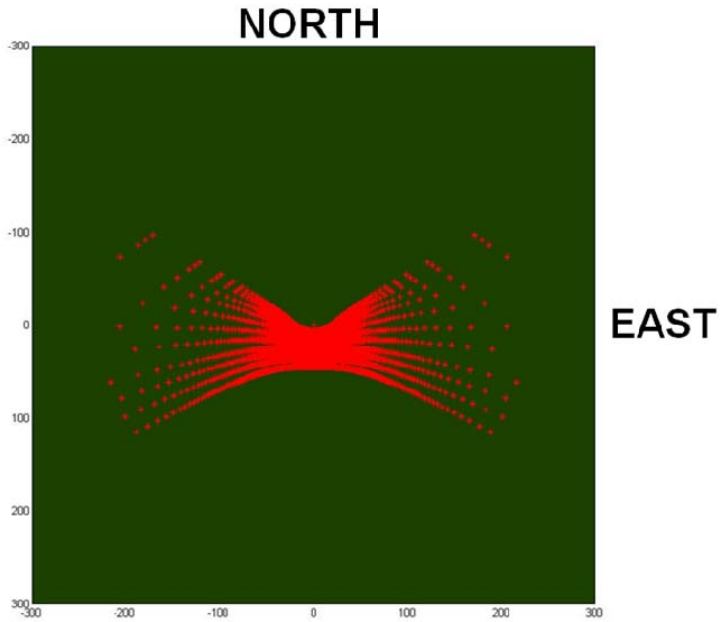

Figure 35: Computational representation of the MIT Briggs field and shadow topography on the ground [TOP VIEW]

Figure 36: Expected topography of shadow flicker effect over the west side of MIT campus for two particular wind turbine sites

The topography of potential shadow flicker throughout the year has been plotted over the west side of MIT campus. Considering the assumptions made earlier, this estimation needs to be viewed as very conservative dealing with the worst possible scenario under the condition of a perfect weather condition and a blade swept area facing the sun light direction in normal direction. Of course, the nacelle is supposed to rotate itself to get aligned with the prevailing wind direction, which is varying over the time. For the more precise computation, those factors need to be taken into account in the future.

The intensity of the shadow of the turbine blade by the way would decrease as the distance increases. In other words, the sharpness of the shadow shedding behind the turbine blade depends on how far it is away from the turbine. Based on the guideline provided by references, at a distance of 10 rotor diameters (equivalent to 37m for *SkyStream3.7*), the human eye should not perceive a wind turbine to be chopping through sunlight, but rather as an object with the sun behind it. In other words, the flicker effect shouldn't be perceivable to the human eye at distances of about 10 rotor diameters, which for the current project is about 37 m in radius and will be named as the actual zone of flicker effect as shown below.

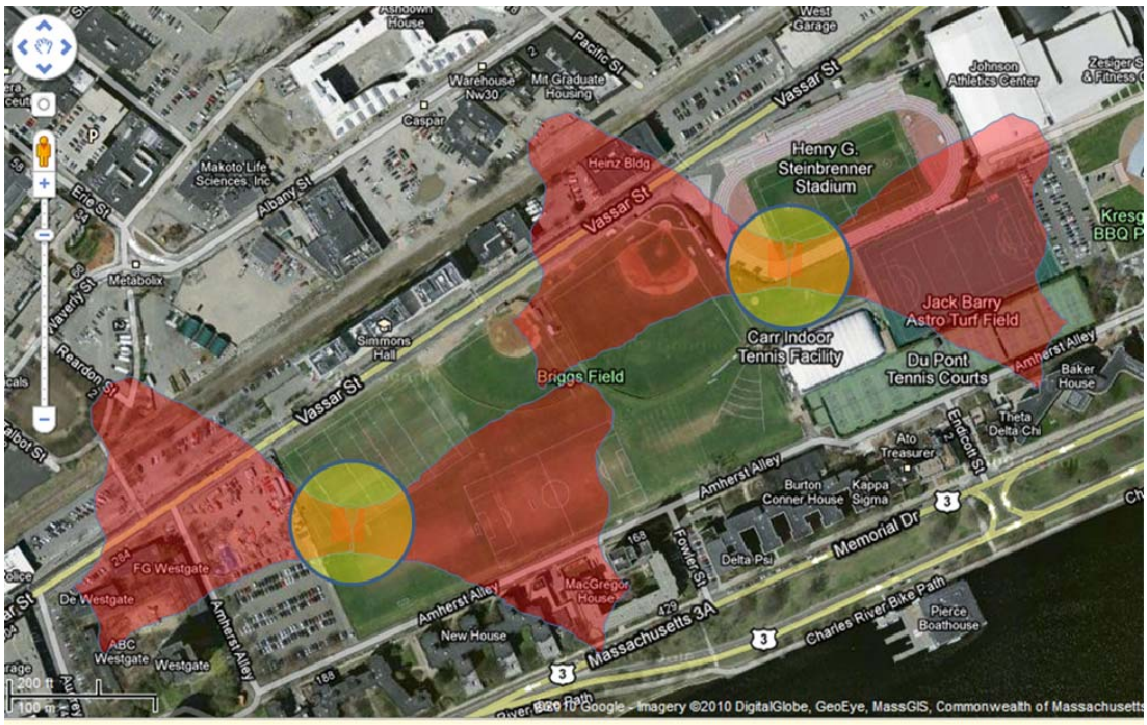

Figure 37: Second flicker plot with sensitive zone demarcation

The red and yellow zone shown above corresponds to the potential zone of shadow effect and actual zone of flicker effect respectively. As clearly seen in the figures above, no building or residential area is exposed to the actual zone of flicker effect.

Sound

Source / Activity	Indicative noise level dB(A)
Threshold of pain	140
Jet aircraft at 250m	105
Pneumatic drill at 7m	95
Truck at 30mph at 100m	65
Busy general office	60
Car at 40mph at 100m	55
SkyStream 3.7 at 10m	40
Quiet bedroom	35
Rural night-time background	20-40
Threshold of hearing	0

Figure 38: level of noise impacts

Figure 39: second representation of noise impacts

*(***Source***: The Sustainable Development Commission (SDC): Wind Power in the UK report)*

Summary and conclusions

Recommendations from the flicker and noise studies are as follows:

- The potential zone of shadow effect is primarily on west-east of the project site resulting in morning-evening shadow effect up to 200m distance from the wind turbine
- The actual zone of shadow flicker effect is limited by 37m in radius
- Shadow flicker cannot be a health or safety issue to the residential area
- Sound level is about 40dB at 10m
- Sound does not appear to be an issue to the residential area

References

[1] *'Wind Energy – The Facts', EWEA, 2009*

[2] *Stankovic, Cambell, Harries. 'The Urban Wind Energy'*

[3]http://www.masstech.org/Project%20Deliverables/Comm_Wind/Fairhaven/Presentation-FairhavenShadow-Acoustic2007-0509.pdf

[4]http://webarchive.nationalarchives.gov.uk/+/http://www.berr.gov.uk//energy/sources/renewables/planning/onshore-wind/shadow-flicker/page18736.html

[5] http://www.sd-commission.org.uk/publications.php?id=234

[6] http://www.dti.gov.uk/renewables/renew_3.5.1.4.htm

[7] *Manzanita Wind Energy Feasibility Study (Final Technical Report), DOE award number: DE-FC36-02GO12111, A000 , 2004*

[8] *Bernhard Voll. The shadow flicker study report, Black springs Wind Farm, energreen wind, 2006*

[9] *Anthony Rogers, Jame Manwell. Wind Turbine Acoustic Noise, Renewable Energy Research Lab., Univ. of Massachuestts at Amherst, 2006*

[10]http://majorprojects.planning.nsw.gov.au/files/1883/Appendix%20C%20Shadow%20flicker%20study.pdf

[11] *Hinweise zur Ermittlung und Beurteilung der optischen Immissionen von Windenergieanlagen (WE-Schatten-Hinweise)*

[12] *Skystream 3.7* specification sheet

[13] Topography from *GoogleEarth.com*

Report Conclusions and Recommendations

No specific recommendations are made by this report since the actual decision on what site to use will be affected by a range of factors, especially economic considerations, which are beyond the scope of this study. The purpose of this report is largely to inform the overall decision process that will be made by MIT facilities. The conclusions of each sub-study on the resource, integration, environmental and community considerations should each be considered independently in terms of informing that decision process.